Rif1 inhibits replication fork progression and controls DNA copy number in Drosophila.

Alexander Munden[1], Zhan Rong[1], Rama Gangula[2], Simon Mallal[2,3] and Jared T. Nordman[1,4]

[1]Dept. of Biological Sciences, Vanderbilt University, Nashville, TN 37232
[2]Dept. of Medicine, [3]Dept. of Pathology, Microbiology and Immunology,
Vanderbilt University School of Medicine, Nashville, TN 37232

Running title: Rif1 controls replication fork progression

Keywords: DNA replication, Common Fragile Sites, Replication Timing, Drosophila, genome stability

[4]Corresponding author: jared.nordman@vanderbilt.edu

ABSTRACT:

Control of DNA copy number is essential to maintain genome stability and ensure proper cell and tissue function. In Drosophila polyploid cells, the SNF2-domain-containing SUUR protein inhibits replication fork progression within specific regions of the genome to promote DNA underreplication. While dissecting the function of SUUR's SNF2 domain, we identified a physical interaction between SUUR and Rif1. Rif1 has many roles in DNA metabolism and regulates the replication timing program. We demonstrate that repression of DNA replication is dependent on Rif1. Rif1 localizes to active replication forks in an SUUR-dependent manner and directly regulates replication fork progression. Importantly, SUUR associates with replication forks in the absence of Rif1, indicating that Rif1 acts downstream of SUUR to inhibit fork progression. Our findings uncover an unrecognized function of the Rif1 protein as a regulator of replication fork progression.

INTRODUCTION:

Accurate duplication of a cell's genetic information is essential to maintain genome stability. Proper regulation of DNA replication is necessary to prevent mutations and other chromosome aberrations that are associated with cancer and developmental abnormalities (Jackson et al., 2014). DNA replication begins at thousands of cis-acting sites termed origins of replication. The Origin Recognition Complex (ORC) binds to replication origins where, together with Cdt1 and Cdc6, it loads an inactive form of the MCM2-7 replicative helicase (Bell and Labib, 2016). Inactive helicases are phosphorylated by two key kinases, S-CDK and Dbf4-dependent kinase (DDK), which results in the activation of the helicase and recruitment of additional factors to form a pair of bi-directional replication forks emanating outward from the origin of replication (Siddiqui et al., 2013). Although many layers of regulation control the initiation of DNA replication, much less in known about how replication fork progression is regulated.

In metazoans, replication origins are not sequence specific and are likely specified by a combination of epigenetic and structural features (Aggarwal and Calvi, 2004; Cayrou et al., 2011; Eaton et al., 2011; Mesner et al., 2011; Miotto et al., 2016; Remus et al., 2004). Furthermore, replication origins are not uniformly distributed throughout the genome. The result of non-uniform origin distribution is that, in origin-poor regions of the genome, a single replication fork must travel great distances to complete replication. If a replication fork encounters an impediment within a large origin-less region of the genome, then replication will be incomplete, resulting in genome instability (Newman et al., 2013). In fact, origin poor regions of the genome are known to be associated with chromosome fragility and genome

instability (Debatisse et al., 2012; Durkin and Glover, 2007; Letessier et al., 2011; Norio et al., 2005). This highlights the need to regulate both the initiation and elongation phases of DNA replication to maintain genome stability.

DNA replication is also regulated in a temporal manner where specific DNA sequences replicate at precise times during S phase, a process known as the DNA replication timing program. While euchromatin replicates in the early part of S phase, heterochromatin and other repressive chromatin types replicate in the later portion of S phase (Gilbert, 2002; Rhind and Gilbert, 2013). Although the process of replication timing has been appreciated for many years, the underlying molecular mechanisms controlling timing have remained elusive. The discovery of factors that regulate the DNA replication timing program, however, demonstrate that replication timing is an actively regulated process.

Once factor that regulates replication timing from yeast to humans is Rif1 (Rap1-interacting factor 1). Rif1 was initially identified as a regulator of telomere length in budding yeast (Hardy et al., 1992), but this function of Rif1 appears to be specific to yeast (Xu, 2004). Subsequently, Rif1 has been shown to regulate multiple aspects of DNA replication and repair. In mammalian cells, Rif1 has been shown to regulate DNA repair pathway choice by preventing resection of double-strand breaks and favoring non-homologous end joining (NHEJ) over homologous recombination (Chapman et al., 2013; Di Virgilio et al., 2013; Zimmermann et al., 2013). Rif1 from multiple organisms contains a Protein Phosphatase 1 (PP1) interaction motif and Rif1 is

able to recruit PP1 to DDK-activated helicases to inactive them and prevent initiation of replication (Davé et al., 2014; Hiraga et al., 2014; 2017).

In yeasts, flies and mammalian cells, Rif1 has been shown to regulate the replication timing program (Cornacchia et al., 2012; Hayano et al., 2012; Peace et al., 2014; Sreesankar et al., 2015; Yamazaki et al., 2012). The precise mechanism(s) through which Rif1 functions to control replication timing are not fully understood. For example, Rif1 has been show to interact with Lamin and is thought to tether specific regions of the genome to the nuclear periphery (Foti et al., 2015). How this activity is related to Rif1's ability to inactivate helicases together with PP1 in controlling the timing program remains obscure.

Studying DNA replication in the context of development provides a powerful method to understand how DNA replication is regulated both spatially and temporally. Although DNA replication is a highly ordered process, it must be flexible enough to accommodate the changes in S phase length and cell cycle parameters that occur as cells differentiate (Matson et al., 2017). For example, during Drosophila development the length of S phase can vary from ~8 hours in a differentiated mitotic cell to 3-4 minutes during early embryonic cell cycles (Blumenthal et al., 1974; Spradling and Orr-Weaver, 1987). Additionally, many tissues and cell types in Drosophila are polyploid, having multiple copies of the genome in a single cell (Edgar and Orr-Weaver, 2001; Lilly and Duronio, 2005; Zielke et al., 2013).

111 In polyploid cells, copy number is not always uniform throughout the genome (Rudkin, 1969;
112 Hua and Orr-Weaver, 2017; Spradling and Orr-Weaver, 1987). Both heterochromatin and
113 several euchromatic regions of the genome have reduced DNA copy number relative to overall
114 ploidy (Nordman et al., 2011). Underreplicated euchromatic regions of the genome share key
115 features with common fragile sites in that they are devoid of replication origins, late replicating,
116 display DNA damage and are tissue-specific (Andreyeva et al., 2008; Nordman et al., 2014; Sher
117 et al., 2012; Yarosh and Spradling, 2014). The presence of underreplication is conserved in
118 mammalian cells, but the mechanism(s) mammalian cells use to promote underreplication is
119 unknown (Hannibal et al., 2014). In Drosophila, underreplication is an active process that is
120 largely dependent on the Suppressor of Underreplication protein, SUUR (Makunin et al., 2002;
121 Nordman and Orr-Weaver, 2015).
122
123 Understanding how the SUUR protein functions will significantly increase our understanding of
124 the developmental control of DNA replication. The SUUR protein has a recognizable SNF2-like
125 chromatin remodeling domain at its N-terminus, but based on sequence analysis, this domain is
126 predicted to be defective for ATP binding and hydrolysis (Makunin et al., 2002; Nordman and
127 Orr-Weaver, 2015). Outside of the SNF2 domain, SUUR has no recognizable motifs or domains,
128 which has hampered a mechanistic understanding of how SUUR promotes underreplication.
129 Recently, however, SUUR was shown to control copy number by directly reducing replication
130 fork progression (Nordman et al., 2014). SUUR associates with active replication replication
131 forks and while loss of SUUR function results in increased replication fork progression,
132 overexpression of SUUR drastically inhibits replication fork progression without affecting origin

133 firing (Nordman et al., 2014; Sher et al., 2012). These findings, together with previous work
134 showing that loss of SUUR function has no influence on ORC binding (Sher et al., 2012) and that
135 SUUR associates with euchromatin in an S phase-dependent manner (Kolesnikova et al., 2013),
136 further supports SUUR as a direct inhibitor of replication fork progression within specific
137 regions of the genome. The mechanism through which SUUR is recruited to replication forks
138 and how it inhibits their progression remains poorly understood.
139
140 Here we investigate how SUUR is recruited to replication forks and how it inhibits fork
141 progression. We show that localization of SUUR to replication forks, but not heterochromatin, is
142 dependent on its SNF2 domain. We identify a physical interaction between SUUR and the
143 conserved replication factor Rif1. Importantly, we demonstrate that underreplication is
144 dependent on *Rif1*. Critically, we have shown that Rif1 localizes to replication forks in an SUUR-
145 dependent manner, where it acts downstream of SUUR to control replication fork progression.
146 Our findings provide mechanistic insight into the process of underreplication and define a new
147 function for Rif1 in replication control.
148
149
150
151
152
153
154

RESULTS:

The SNF2 domain is essential for SUUR function and replication fork localization

As a first step in understanding the mechanism of SUUR function, we wanted to define how it is localized to replication forks. SUUR has only one conserved domain: a SNF2-like domain in its N-terminal region that is predicted to be defective for ATP binding and hydrolysis (Makunin et al., 2002; Nordman and Orr-Weaver, 2015). To study the function of SUUR's SNF2 domain, we generated a mutant in which the SNF2 domain was deleted and the resulting mutant protein was expressed under the control of the endogenous *SuUR* promoter. This mutant, $SuUR^{\Delta SNF}$, was then crossed to an *SuUR* null mutant so that it was the only form of the the SUUR protein present. We tested the function of the $SuUR^{\Delta SNF}$ mutant protein by assessing its ability to promote underreplication in the larval salivary gland. We purified genomic DNA from larval salivary glands isolated from wandering 3rd instar larvae and generated genome-wide copy number profiles using Illumina-based sequencing. We compared the results we obtained from the $SuUR^{\Delta SNF}$ mutant to copy number profiles from wild-type (WT) and *SuUR* null mutant salivary glands. To identify underreplicated domains, we used CNVnator, which identifies copy number variants (CNVs) based on a statistical analysis of read depth (Abyzov et al., 2011). To be called as underreplicated, regions must not be called as underreplicated in 0-2 hour embryo samples that have uniform copy number and must be larger than 10kb.

The effect of deleting the SNF2 domain was qualitatively and quantitatively similar to the *SuUR* null mutant. Qualitatively, underreplication was suppressed in the $SuUR^{\Delta SNF}$ mutant and the copy number profile was similar to the *SuUR* null mutant (Figure 1B and Supplemental Figure

177 1). Quantitatively, out of the 90 underreplicated sites identified in WT salivary glands, 59 were
178 not detected in the *SuUR*$^{\Delta SNF}$ mutant (Supplementary Table 1) and copy number was
179 significantly increased in the euchromatic underreplicated domains similar to the *SuUR* null
180 mutant (Figure 1C). We validated our deep-sequencing findings using quantitative droplet
181 digital PCR (ddPCR) at four underreplicated domains (Figure 1D). Our findings show that the
182 SNF2-like domain of SUUR is necessary to promote underreplication.
183
184 To determine if the SUUR$^{\Delta SNF}$ protein was still able to associate with chromatin, we localized
185 SUUR and the SUUR$^{\Delta SNF}$ mutant proteins in ovarian follicle cells. During follicle cell
186 development, these cells undergo programmed changes in their cell cycle and DNA replication
187 programs (Claycomb and Orr-Weaver, 2005; Hua and Orr-Weaver, 2017). At a precise time in
188 their differentiation program, follicle cells cease genomic replication and amplify six defined
189 sites of their genome through a re-replication based mechanism. Early in this gene amplification
190 process, both initiation and elongation phases of replication are coupled. Later in the process,
191 however, initiation no longer occurs and active replication forks can be visualized by pulsing
192 amplifying follicle cells with 5-ethynyl-2'deoxyuridine (EdU) (Claycomb et al., 2002). Active
193 replication forks resolve into a double-bar structure, where each bar represents a series of
194 active replication forks travelling away from the origin of replication (Claycomb and Orr-
195 Weaver, 2005). By monitoring SUUR localization in amplifying follicle cells, we can
196 unambiguously determine if SUUR associates with active replication forks.
197

198 SUUR has two distinct modes of chromatin association during the endo cycle. It constitutively
199 localizes to heterochromatin and dynamically associates with replication forks (Kolesnikova et
200 al., 2013; Nordman et al., 2014; Swenson et al., 2016). In agreement with previous studies,
201 SUUR localized to both replication forks and heterochromatin in amplifying follicle cells (Figure
202 1E) (Nordman et al., 2014). In contrast, the SUUR$^{\Delta SNF}$ mutant localized to heterochromatin, but
203 its recruitment to active replication forks was severely reduced (Figure 1E). Together, these
204 results demonstrate that the SNF2 domain is important for SUUR recruitment to replication
205 forks and is essential for SUUR-mediated underreplication.
206
207 **SUUR associates with Rif1**
208 Interestingly, overexpression of the SNF2 domain and C-terminal portion of SUUR have
209 different underreplication phenotypes. Whereas overexpression of the C-terminal two-thirds of
210 SUUR promotes underreplication (Kolesnikova et al., 2005), overexpression of the SNF2 domain
211 suppresses underreplication in the presence of endogenous SUUR (Kolesnikova et al., 2005).
212 The C-terminal region of SUUR, however, has no detectable homology or conserved domains
213 (Makunin et al., 2002). These observations, together with our own results demonstrating that
214 the SNF2 domain of SUUR is responsible its localization to replication forks, led us to
215 hypothesize that SUUR is recruited to replication forks through its SNF2 domain where it could
216 recruit an additional factor(s) through its C-terminus to inhibit replication fork progression.
217
218 To test the hypothesis that a critical factor interacts with the C-terminal region of SUUR to
219 promote underreplication, we used immunoprecipitation mass spectrometry studies to identify

SUUR-interacting proteins. We generated flies that expressed FLAG-tagged full length SUUR or the SNF2 domain of SUUR, immunoprecipitated these constructs and identified associated proteins through mass spectrometry. If SUUR recruits a factor to replication forks outside of its SNF2 domain, then we would expect this factor to be present only in full length purifications and not in the SNF2 domain purification. A single protein fulfilled this criteria: Rif1 (Table 1). This result raises the possibility Rif1 works together with SUUR to inhibit replication fork progression.

Underreplication is dependent on Rif1

If SUUR recruits Rif1 to replication forks to promote underreplication, then underreplication should be dependent on *Rif1*. To test this hypothesis, we used CRISPR-based mutagenesis to generate *Rif1* null mutants in Drosophila (Bassett et al., 2013; Gratz et al., 2013) (Figure 2A). Western blot analysis of ovary extracts from two deletion mutants, $Rif1^{1}$ and $Rif1^{2}$, show no detectable Rif1 protein (Supplemental Figure 2A). Also, no signal was detected in the $Rif1^{1}/Rif1^{2}$ mutant by immunofluorescence (Supplemental Figure 2B). The $Rif1^{1}/Rif1^{2}$ null mutant was viable and fertile showing only a modest defect in embryonic hatch rate relative to wild-type flies with a 92% hatch rate for wild type embryos vs. 88% for the $Rif1^{1}/Rif^{2}$ mutant embryos (Supplemental Figure 2C). This is in contrast to a previous a study reporting *Rif1* is essential in Drosophila (Sreesankar et al., 2015). Rif1's essentiality, however, was based on RNAi and not a mutation of the *Rif1* gene (Sreesankar et al., 2015). The most likely explanation for this discrepancy is that the lethality in the RNAi experiments was due to an off-target effect.

To determine if *Rif1* is necessary for underreplication, we dissected salivary glands from *Rif1*^{1}/*Rif1*^{2} (herein referred to as *Rif1*$^{-}$) heterozygous larvae and extracted genomic DNA for Illumina-based sequencing to measure changes in DNA copy number. Strikingly, underreplication is abolished upon loss of Rif1 function (Figure 2B and C; Supplemental Figure 3). We validated our sequence-based copy number assays with quantitative PCR at a subset of underreplicated regions using ddPCR (Figure 2D). Furthermore, we determined the read density at all euchromatic sites of underreplication called in our wild-type samples, which quantitatively demonstrates that Rif1 is essential for underreplication (Figure 2C). These results demonstrate that underreplication is dependent on *Rif1*.

It is possible that the *Rif1* mutant indirectly influences underreplication through changes in replication timing. Underreplicated domains, both euchromatic and heterochromatic, tend to be late replicating regions of the genome (Belyaeva et al., 2012; Makunin et al., 2002). Therefore, if these regions replicated earlier in S phase in a *Rif1* mutant, then this change could prevent their underreplication. In fact, SUUR associates with late replicating regions of the genome (Filion et al., 2010; Pindyurin et al., 2007). Due to their large polyploid nature, salivary glands cells cannot be sorted to perform genome-wide replication timing experiments. Because heterochromatin replicates exclusively in late S phase, however, late replication can be visualized when EdU is incorporated exclusively in regions of heterochromatin. To assess if *Rif1* mutants have a clear pattern of late replication in larval salivary glands, we isolated salivary glands from early 3rd instar larvae, which are actively undergoing endo cycles. We pulsed these salivary glands with EdU to visualize sites of replication and co-stained with an anti-HP1

antibody to mark heterochromatin. In wild-type salivary glands, only rarely (1 of 238 EdU^+ cells; 0.4%) did we detect EdU incorporation in regions of heterochromatin (Supplemental Figure 4). This is consistent with the lack of heterochromatin replication due to underreplication. In contrast, in both *SuUR* and *Rif1* mutants, we could readily detect cells that were solely incorporating EdU within regions of heterochromatin (32 of 327 EdU^+ cells; 9.8% for *SuUR* and 70 of 385 EdU^+ cells; 18.2% for *Rif1*) (Supplemental Figure 4). Therefore, we conclude that *Rif1* mutants still have a clear pattern of late replication. Given that heterochromatin underreplication is suppressed in a *Rif1* mutant, although it is still late replicating, indicates that replication timing cannot solely explain the lack of underreplication associated with loss of Rif1 function.

While characterizing Rif1's role in underreplication and patterns of DNA replication in endo cycling cells, we did observe differences in the heterochromatic regions of *SuUR* and *Rif1* mutants. First, although underreplication is suppressed in both mutants (Figure 2 and Supplemental Figure 3), the chromocenters were abnormally large in *Rif1* mutant relative to an *SuUR* mutant as observed by DAPI staining consistent with the 'fluffy' enlarged chromocenters seen in Rif1 mutant mouse cells (Supplemental Figure 4) (Cornacchia et al., 2012). Although, this phenotype was present in all endo cycling cells, it was especially dramatic in the ovarian nurse cells (Supplemental Figure 5). Second, Illumina-based copy number profiles revealed an increase in copy number in some pericentric heterochromatin regions in the *Rif1* mutant relative to the *SuUR* mutant (Supplemental Figure 3). Collectively, these results suggest that heterochromatin is partially, but not fully replicated in *SuUR* mutant endo cycling cells,

286 consistent with previous cytological analysis (Demakova et al., 2007). In contrast, loss of Rif1
287 function appears to completely restore heterochromatic replication in endo cycling cells.
288
289 **Rif1 affects replication fork progression.**
290 SUUR-mediated underreplication occurs through inhibition of replication fork progression
291 (Nordman et al., 2014; Sher et al., 2012). If SUUR acts together with Rif1 to promote
292 underreplication, then Rif1 is expected to control replication fork progression. DNA combing
293 assays in human and mouse cells from multiple groups have come to different conclusions as to
294 whether Rif1 affects replication fork progression (Alver et al., 2017; Cornacchia et al., 2012;
295 Hiraga et al., 2017; Yamazaki et al., 2012). Rif1, however, has been shown to be associated with
296 replication forks through nascent chromatin capture, an iPOND-like technique used to isolate
297 proteins associated with active replication forks (Alabert et al., 2014). To determine directly if
298 Rif1 controls replication fork progression, we performed copy number assays on amplifying
299 follicle cells.
300
301 Gene amplification in ovarian follicle cells occurs at six discrete sites in the genome through a
302 re-replication based mechanism. Copy number profiling of these amplified domains provides a
303 quantitative assessment of the number of rounds of origin firing and the distance replication
304 forks have travelled during the amplification process, allowing us to disentangle the initiation
305 and elongation phases of DNA replication. To determine if Rif1 affects origin firing and/or
306 replication fork progression, we isolated wild-type and *Rif1* mutant stage 13 egg chambers,
307 which represent the end point of the amplification process, and made quantitative DNA copy

number measurements. Loss of Rif1 function resulted in an increase in replication fork progression without significantly affecting copy number at the origin of replication at all sites of amplification (Figure 3A).

To quantify the changes in fork progression we observed at sites of amplification, we computationally determined the peak of amplification and the region on each arm of the amplified domain that represents one half of the copy number at the highest point of the amplicon (Nordman et al., 2014). This quantitative analysis of origin firing and replication fork progression revealed that origin firing was not affected in the *Rif1* mutant, as no major change in copy number was detected at the origin of replication when comparing wild type and *Rif1* mutant stage 13 follicle cells (Supplemental Table 2). In contrast, the width of each replication gradient, which represents the rate of fork progression, was significantly increased at all sites of amplification (Figure 3A; Supplemental Table 2). Based on the observation that the *Rif1* mutant does not affect origin firing, but specifically affects the distance replication forks travel during the gene amplification process, we conclude that Rif1 regulates replication fork progression.

Given that the *Rif1* mutant phenocopies an *SuUR* mutant with respect to replication fork progression, we next wanted to determine the cause of increased replication fork progression at amplified loci upon loss of Rif1 function. Previously, it was shown that a prolonged period of gene amplification in the *SuUR* mutant gives rise to the extended replication gradient at sites of amplification (Nordman et al., 2014). Gene amplification starts synchronously in all follicle cells at stage 10B of egg chamber development (Calvi et al., 1998). By the end of gene amplification,

however, only a subset of follicle cells display visual amplification foci as judged by EdU incorporation (Nordman et al., 2014). To determine if Rif1 controls replication fork progression by increasing the period of gene amplification comparable to an *SuUR* mutant , we quantified the fraction of stage 13 follicle cells that were EdU positive. Similar to an *SuUR* mutant, loss of Rif1 function also resulted in a prolonged period of EdU incorporation with 34% of follicle cells visibly incorporating EdU in wild type follicle cells, 100% in an *SuUR* mutant and 98.5% in the *Rif1* mutant (Figure 3B). This results suggests that Rif1 has a destabilizing effect on replication forks, resulting in a premature cessation of replication fork progression.

Rif1 acts downstream of SUUR

Rif1 could control SUUR activity and underreplication by at least two different mechanisms. Rif1 could act upstream of SUUR and directly or indirectly regulate SUUR's ability to associate with chromatin. For example, Histone H1 and HP1 affect underreplication by influencing SUUR's ability to associate with chromatin (Andreyeva et al., 2017; Pindyurin et al., 2008). Alternatively, Rif1 could act downstream of SUUR to control replication fork progression. We sought to distinguish between these possibilities by determining whether SUUR could still associate with replication forks in the absence of Rif1 function.

To monitor SUUR's association with heterochromatin and replication forks in the same cell type, we localized SUUR in amplifying follicle cells where replication forks (double bars) and heterochromatin (chromocenter) can be visualized unambiguously, in the presence and absence of Rif1. SUUR localized to both replication forks and heterochromatin in the absence of

352 Rif1 function (Figure 4). Therefore, we conclude that Rif1 acts downstream of SUUR to inhibit
353 fork progression and that SUUR lacks the ability to inhibit replication fork progression in the
354 absence of Rif1.
355
356 **Rif1 localizes to active replication forks.**
357 Although our genetic data indicate that Rif1 affects replication fork progression, we wanted to
358 determine if Rif1 controls replication fork progression through a direct or indirect mechanism. If
359 Rif1 directly influences replication fork progression and/or stability, then it should localize to
360 active replication forks. To assess this possibility, we visualized Rif1 localization during gene
361 amplification in follicle cells using a Rif1-specific antibody (Supplemental Figure 2).
362 Rif1 localization pattern was strikingly similar to that of SUUR. First, Rif1 is localized to
363 heterochromatin in all amplification stages amplifying follicle cells (Figure 5). Second, Rif1
364 localized to sites of amplification even prior to the formation of double bar structures, with
365 weak staining in early stage follicle cells and more intense staining as amplification progressed.
366 Third, in the later stages of gene amplification Rif1 was localized to active replication forks.
367 Taken together, these results demonstrate that Rif1 dynamically associates with the replication
368 forks to regulate their progression.
369
370 **SUUR is required to retain Rif1 at replication forks.**
371 Based on our observations that SUUR physically associates with Rif1 and that a *Rif1* mutant
372 phenocopies an *SuUR* mutant, we hypothesized that SUUR recruits a Rif1/PP1 complex to
373 replication forks. If true, then Rif1 association with replication forks should be at least partially

374 dependent on SUUR. To test this hypothesis, we monitored the localization of Rif1 in *SuUR*
375 mutant amplifying follicle cells. We found that Rif1's association with replication forks was
376 largely dependent on SUUR, as the Rif1 signal was lost in late stage amplifying follicle cells in an
377 *SuUR* mutant (Figure 5). Rif1's recruitment to replication foci, however, was not completely
378 dependent on SUUR. In a subset of stage 10B and 11 egg chambers, when both initiation of
379 replication and fork progression are still coupled, we observed Rif1 localization to amplification
380 foci in a subset of follicle cells (data not shown). Rif1 staining was lost, however, in stage 12 and
381 13 egg chambers. We conclude that while the initial recruitment of Rif1 to sites of amplification
382 is not completely dependent on SUUR, SUUR is necessary to retain Rif1 at replication forks.
383
384 **The PP1-interacting motif of Rif1 is necessary for underreplication**
385 Because Rif1 is known to recruit PP1 to replication origins to regulate initiation, this led us to
386 ask if the same interaction between Rif1 and PP1 is important for Rif1's regulation of replication
387 fork progression. Rif1 associates with Protein Phosphatase 1 (PP1) through a conserved
388 interaction motif, thereby recruiting PP1 to MCM complexes and inactivating them (Davé et al.,
389 2014; Hiraga et al., 2017; 2014). Based on this model of Rif1 function, we wanted to determine
390 if Rif1's ability to interact with PP1 was necessary for Rif1-mediated underreplication. We used
391 CRISPR-based mutagenesis to mutate the conserved SILK/RSVF PP1 interaction motif to
392 SAAK/RASA. Western blot analysis showed that mutation of the SILK/RSVF motif did not affect
393 protein stability (Supplemental Figure 6). Mutation of this motif has been shown to disrupt the
394 Rif1/PP1 interaction in organisms from yeast to humans (Alver et al., 2017; Davé et al., 2014;
395 Hiraga et al., 2017; 2014; Mattarocci et al., 2014; Sreesankar et al., 2015; Sukackaite et al.,

2017). We isolated salivary glands from *Rif1*^{PP1} mutant wandering 3rd instar larvae, extracted DNA and measured the copy number of multiple underreplicated domains. Similar to the *Rif1* mutant, underreplication was completely abolished in the *Rif1*^{PP1} mutant (Figure 6A). Thus, a Rif1/PP1 complex is necessary to promote underreplication.

DISCUSSION:

The SUUR protein is responsible for promoting underreplication of heterochromatin and many euchromatin regions of the genome. Although SUUR was recently shown to promote underreplication through inhibition of replication fork progression, the underlying molecular mechanism has remained unclear. Through biochemical, genetic, genomic and cytological approaches, we have found that SUUR recruits Rif1 to replication forks and that Rif1 is responsible for underreplication. This model is supported by several independent lines of evidence. First, SUUR physically associates with Rif1, and SUUR and Rif1 co-localize at sites of replication. Second, underreplication is dependent on Rif1, although Rif1 mutants have a clear pattern of late replication in endo cycling cells. Third, SUUR localizes to replication forks and heterochromatin in a *Rif1* mutant, however, it is unable to inhibit replication fork progression in the absence of Rif1. Fourth, Rif1 directly controls replication fork progression and phenocopies the effect loss of SUUR function has on replication fork progression. Fifth, SUUR is required for Rif1 localization to replication forks. Critically, using the gene amplification model to separate initiation and and elongation of replication, we have shown that Rif1 can affect fork progression

417 without altering the extent of initiation. Based on these observations, we have defined a new
418 function of Rif1 as a direct regulator of replication fork progression.
419
420 ***SNF2 domain and fork localization***
421 Our work suggests that the SNF2 domain of SUUR is critical for its ability to localize to
422 replication forks. This is based on the observation that deletion of this domain results in a
423 protein that is unable to localize to replication forks, but still localizes to heterochromatin.
424 SUUR has previously been shown to dynamically localize to replication forks during S phase, but
425 constitutively binds to heterochromatin (Kolesnikova et al., 2013; Nordman et al., 2014). SUUR
426 associates with HP1 and this interaction occurs between the central region of SUUR and HP1.
427 (Pindyurin et al., 2008). Therefore, we speculate that the interaction between SUUR and HP1 is
428 responsible for constitutive SUUR localization to heterochromatin, while a different interaction
429 between the SNF2 domain and a yet to be defined component of the replisome, or replication
430 fork structure itself, recruits SUUR to active replication forks during S phase.
431
432 Uncoupling of SUUR's ability to associate with replication forks and heterochromatin also
433 provides a new level of mechanistic understanding of underreplication. Overexpression of the
434 C-terminal two-thirds of SUUR is capable of inducing ectopic sites of underreplication. In
435 contrast, overexpression of the SUUR's SNF2 domain, in the presence of endogenous SUUR,
436 suppresses SUUR-mediated underreplication (Kolesnikova et al., 2005). Together with the data
437 presented here, we suggest that overexpression of the SNF2 domain interferes with
438 recruitment of full-length SUUR to replication forks, by saturating potential SUUR binding sites

439 at the replication fork. Although the C-terminal region of SUUR is necessary to induce
440 underreplication (Kolesnikova et al., 2005), the C-terminal portion of SUUR remains associated
441 with heterochromatin in the SuUR$^{\Delta SNF}$ construct , but this protein is not sufficient to induce
442 underreplication. We suggest that at physiological levels, the affinity of SUUR with replication
443 forks is substantially diminished in the absence of the SNF2 domain. Our work raises questions
444 about the biological significance of SUUR binding to heterochromatin, since without the SNF2
445 domain SUUR is still constitutively bound to heterochromatin, yet unable to induce
446 underreplication. Additionally, SUUR dynamically associates with heterochromatin in mitotic
447 cells although heterochromatin is fully replicated (Swenson et al., 2016).
448
449 ***Rif1 controls underreplication***
450 While trying to uncover the molecular mechanism through which SUUR is able to inhibit
451 replication fork progression, we have uncovered a physical interaction between SUUR and Rif1.
452 Through subsequent analysis, we demonstrated that Rif1 has a direct role in copy number
453 control and that Rif1 acts downstream of SUUR in the underreplication process. Although
454 underreplication is largely dependent on SUUR, there are several sites that display a modest
455 degree of underreplication in the absence of SUUR (Demakova et al., 2007; Sher et al., 2012). In
456 a Rif1 mutant, however, these sites are fully replicated and there is no longer any detectable
457 levels of underreplication within any regions of the genome. It is possible that Rif1 is capable of
458 promoting underreplication through a mechanism independent of SUUR. Therefore, we
459 conclude that Rif1 is a critical factor in driving underreplication.
460

Further emphasizing the critical role Rif1 plays in copy number control, we have shown that Rif1 acts downstream of SUUR in promoting underreplication. SUUR is still able to associate with chromatin in the absence of Rif1, but is unable to promote underreplication. Underreplicated regions of the genome, including heterochromatin, tend to be late replicating, raising the possibility that changes in replication timing in a *Rif1* mutant suppresses underreplication. *Rif1* mutant endo cycling cells of Drosophila display a cytological pattern of late replication, where heterochromatin is discretely replicated. While Rif1 is likely to control replication timing in Drosophila, we argue that the changes in copy number associated with loss of Rif1 function are not solely due to a loss of late replication. This is supported by the clear pattern of late replication of heterochromatin in *Rif1* mutant endo cycling cells, although heterochromatin appears to be fully replicated in these cells. Previous work in mammalian polyploid cells has shown that underreplication is dependent on Rif1, which was attributed to changes in replication timing (Hannibal and Baker, 2016). It is important to note that Rif1-dependent changes in replication timing were not measured in this system and that many genomic regions transition from early to late replication in a *Rif1* mutant (Foti et al., 2015). Our work raises the possibility that Rif1 has a direct role in mammalian underreplication through a mechanism similar to that of Drosophila and may not simply be due to indirect changes in replication timing. Future work will be necessary to define the role of mammalian Rif1 in underreplication.

Rif1 regulates replication fork progression

Our analysis of amplification loci demonstrates that Rif1 controls replication fork progression independently of initiation control, thus demonstrating that Rif1 has a specific effect on

483 replication fork progression. Therefore, we have uncovered a new role for Rif1 in DNA
484 metabolism as a regulator of replication fork progression. Rif1 has been identified as part of the
485 replisome in human cells by nascent chromatin capture, a technique that identifies proteins
486 associated with newly synthesized chromatin (Alabert et al., 2014). Multiple studies have
487 assessed whether loss of Rif1 function affects replication fork progression in yeast, mouse and
488 human cells, but have come to different conclusions (Alver et al., 2017; Cornacchia et al., 2012;
489 Hiraga et al., 2017; Yamazaki et al., 2012). DNA fiber assays have been used to measure fork
490 progression in these studies and nearly all have shown that *Rif1* mutants have a slight increase
491 in replication fork progression although not always statistically significant. There could be
492 several reasons for these differing results; Rif1 may control replication fork progression in
493 specific genomic regions that may be underrepresented in some assays, Rif1 function could
494 vary among different cell types, or sample sizes may have been too small to reach significance.
495 Our observations, taken together with these previous studies, leave open the possibility that
496 Rif1-mediated control of replication fork progression could be an evolutionarily conserved
497 function of Rif1. We do not suggest that Rif1 is constitutively associated with replication forks in
498 all cell types. Rather, Rif1 could be recruited to replication forks at a specific time in S phase, or
499 in specific developmental contexts, to modulate the progression of replication forks and
500 provide an additional layer of regulation of the DNA replication program.
501
502 How could SUUR and Rif1 function in concert to inhibit replication fork progression? We have
503 shown that Rif1 retention at replication forks is dependent on SUUR. Additionally,
504 underreplication depends on Rif1's ability to interact with PP1. Rif1/PP1 dephosphorylates

DDK-activated helicases to control replication initiation (Davé et al., 2014; Hiraga et al., 2017; 2014). More recently, however, DDK-phosphorylated MCM subunits were shown to be necessary to maintain CMG association and stability of the helicase (Alver et al., 2017). This result suggests that continued phosphorylation of the helicase is necessary for replication fork progression (Alver et al., 2017). We propose that SUUR recruits Rif1/PP1 to replication forks where it is able to dephosphorylate MCM subunits, ultimately inhibiting replication fork progression. Although this mechanism needs to be tested biochemically, it provides a framework to address the underlying molecular mechanism responsible for controlling DNA copy number and could provide new insight into the mechanism(s) Rif1 employs to regulate replication timing.

MATERIALS AND METHODS

Strain list:

WT – Oregon R

SuUR^{-} – *w*^{118}; *SuUR*^{ES}

SuUR$^{\Delta SNF}$ – *SuUR*^{ES}, *PBac*{w^{+} *SuUR*$^{\Delta SNF}$}

Rif1^{-} – *w*^{118}; *Rif1*^{1} / *Rif1*^{2}

Rif1^{PP1} – *w*^{118}; *Rif1*^{PP1}

BAC-mediated recombineering:

BAC-mediated recombineering (Sharan et al., 2009) was used to delete the portion of the *SuUR* gene corresponding to the SNF2 domain. An *attB-P[acman]* clone with a 21-kb genomic region containing the *SuUR* and a *galK* insertion in the *SuUR* coding region (described in (Nordman et al., 2014)) was used as a starting vector. Next, a gene block (IDT) was used to replace the gal*K* cassette and generate a precise deletion within the *SuUR* gene. The resulting vector was verified by fingerprinting, PCR and sequencing. The *SuUR*$^{\Delta SNF}$ BAC was injected into a strain harboring the *86F8* landing site (Best Gene Inc.).

Generation of heat shock-inducible, FLAG tagged SuUR transgenic lines:

The portion of the *SuUR* gene encoding the SNF2 domain (amino acids 1 to 278) was fused to the SV40 NLS (Barolo et al., 2000) and a 3X-FLAG tag sequence was added to the 5’ end of *SuUR SNF2* sequence. The resulting construct was cloned into the pCaSpeR-hs vector (Thummel and

549 Pirrotta, V.: Drosophila Genomics Resource Center) using the NotI and XbaI restriction sites. A
550 3X-FLAG tag sequence was added to the 5' end of of the *SuUR* coding region and cloned into
551 the pCaSpeR-hs vector also using the NotI and XbaI restriction sites. The resulting constructs
552 were verified by sequencing and injected into a w^{1118} strain (Best Gene Inc.).
553
554 *CRISPR mutagenesis:*
555 To generate null alleles of *Rif1*, gRNAs targeting the 5' and 3' ends of the *Rif1* gene were cloned
556 into the pU6-BbsI plasmid as described (Gratz et al., 2015) using the DRSC Find CRISPRs tool
557 (http://www.flyrnai.org/crispr2/index.html). Both gRNAs were co-injected into a *nos-Cas9*
558 expression stock (Best Gene Inc.). Surviving adults were individually crossed to *CyO*/*Tft*
559 balancer stock and *CyO*-balanced progeny were screened by PCR for a deletion of the *Rif1*
560 locus. Stocks harboring a deletion were further characterized by sequencing. Both $Rif1^{1}$ and
561 $Rif1^{2}$ mutants had substantial deletions of the *Rif1* gene and both had frame shift mutations
562 early in the coding region. $Rif1^{1}$ has a frame shift mutation at amino acid 14, whereas $Rif1^{2}$ has
563 a frame shift mutation at amino acid 11.
564
565 To generate a *Rif1* allele defective for PP1 binding, the pU6-BbsI vector expressing the gRNA
566 targeting the 3' end of *Rif1* was co-injected with a recovery vector that contained the
567 mutagenized SILK and RVSV (SAAK and RASA) sites with 1kb of homology upstream and
568 downstream of the mutagenized region. Surviving adults were crossed as above and screened
569 by sequencing.
570

571 *Cytological analysis and microscopy:*

572 Ovaries were dissected from females fattened for two days on wet yeast in Ephrussi Beadle
573 Ringers (EBR) medium (Beadle and Ephrussi, 1935). Ovaries were pulsed with 5-ethynyl-2-
574 deoxyuridine (EdU) for 30 minutes, fixed in 4% formaldehyde and prepared for
575 immunofluorescence (IF) as described (Nordman et al., 2014).

576

577 For IF using both anti-Rif1 and anti-SUUR antibodies, ovaries were dissected, pulsed with 50µM
578 EdU and fixed. Ovaries were then incubated in primary antibody (1:200) overnight at 4^{o}C. Alexa
579 Fluor secondary antibodies (ThermoFisher) were used at a dilution of 1:500 for 2 hours at room
580 temperature. EdU detection was performed after incubation of the secondary antibody using
581 Click-iT Alexa Fluor-555 or -488 (Invitrogen). All images were obtained using a Nikon Ti-E
582 inverted microscope with a Zyla sCMOS digital camera. Images were deconvolved and
583 processed using NIS-Elements software (Nikon).

584

585 For salivary gland IF, 3rd instar larvae were collected prior to the wandering stage. Salivary
586 glands were dissected in EBR, pulsed with 50µM EdU for 30 minutes and fixed with 4%
587 formaldehyde. Salivary glands were incubated in anti-HP1 antibody (Developmental Studies
588 Hybridoma Bank; C1A9) overnight at 4^{o}C. Alexa Fluor secondary antibodies staining and Click-iT
589 EdU labeling were performed as described above.

590

591 *Rif1 antibody production:*

592 Rif1 antiserum was produced in guinea pigs and rabbits (Cocalico Biologicals Inc.). Briefly, a Rif1
593 protein fragment from residues 694-1094 (Sreesankar et al., 2012) was C-terminally six-
594 histidine tagged and and expressed in *E. coli* Rossetta DE3 cells and purified using Ni-NTA
595 Agarose beads (Qiagen). The purified protein was used for injection (Cocalico Biologicals Inc.)
596 and serum was affinity purified as described (Moore and Orr-Weaver, 1998). Affinity purified
597 guinea pig anti-Rif1 antibody was used for immunofluorescence.
598
599 *IP-mass spec:*
600 Flies containing heat shock-inducible *SuUR* transgenes were expanded into population cages. 0-
601 24 hour embryos were collected, incubated at 37^{o}C for one hour, and allowed to recover for
602 one hour following heat shock treatment. Wild-type embryos were used as a negative control.
603 Embryos were dechorionated in bleach and fixed for 20 minutes in 2% formaldehyde.
604 Approximately 0.5g of fixed and dechorionated embryos were used for each replicate. Embryos
605 were disrupted by douncing in Buffer 1 (Shao et al., 1999), followed by centrifugation at 3,000 x
606 g for 2 minutes at 4^{o}C and resuspended in lysis buffer 3 (MacAlpine et al., 2010) . Chromatin
607 was prepared by sonicating nuclei for a total of 40 cycles of 30" ON and 30" OFF at max power
608 using a Bioruptor 300 (Diagnenode) with vortexing and pausing after every 10 cycles. Cleared
609 lysates were incubated with anti-FLAG M2 affinity gel (Sigma) for 2 hours at 4^{o}C. After extensive
610 washing in LB3 and LB3 with 1M NaCl, proteins were eluted using 3X FLAG peptide (Sigma).
611 Crosslinks were reversed by boiling purified material in Laemmli buffer with β-mercaptoethanol
612 for 20 minutes.
613

Immunoprecipitated samples were separated on a 4-12% NuPAGE Bis-Tris gel (Invitrogen), proteins were stained with Novex colloidal Coomassie stain (Invitrogen), and destained in water. Coomassie stained gel regions were cut from the gel and diced into $1mm^3$ cubes. Proteins were reduced and alkylated, destained with 50% MeCN in 25mM ammonium bicarbonate, and in-gel digested with trypsin (10ng/uL) in 25mM ammonium bicarbonate overnight at 37°C. Peptides were extracted by gel dehydration with 60% MeCN, 0.1% TFA, the extracts were dried by speed vac centrifugation, and reconstituted in 0.1% formic acid. Peptides were analyzed by LC-coupled tandem mass spectrometry (LC-MS/MS). An analytical column was packed with 20cm of C18 reverse phase material (Jupiter, 3 µm beads, 300Å, Phenomenox) directly into a laser-pulled emitter tip. Peptides were loaded on the capillary reverse phase analytical column (360 µm O.D. x 100 µm I.D.) using a Dionex Ultimate 3000 nanoLC and autosampler. The mobile phase solvents consisted of 0.1% formic acid, 99.9% water (solvent A) and 0.1% formic acid, 99.9% acetonitrile (solvent B). Peptides were gradient-eluted at a flow rate of 350 nL/min, using a 120-minute gradient. The gradient consisted of the following: 1-3min, 2% B (sample loading from autosampler); 3-98 min, 2-45% B; 98-105 min, 45-90% B; 105-107 min, 90% B; 107-110 min, 90-2% B; 110-120 min (column re-equilibration), 2% B. A Q Exactive HF mass spectrometer (Thermo Scientific), equipped with a nanoelectrospray ionization source, was used to mass analyze the eluting peptides using a data-dependent method. The instrument method consisted of MS1 using an MS AGC target value of 3e6, followed by up to 15 MS/MS scans of the most abundant ions detected in the preceding MS scan. A maximum MS/MS ion time of 40 ms was used with a MS2 AGC target of 1e5. Dynamic exclusion was set to 20s, HCD collision energy was set to 27 nce, and peptide match and isotope

636 exclusion were enabled. For identification of peptides, tandem mass spectra were searched
637 with Sequest (Thermo Fisher Scientific) against a *Drosophila melanogaster* database created
638 from the UniprotKB protein database (www.uniprot.org). Search results were assembled using
639 Scaffold 4.3.4 (Proteome Software).
640
641 *Genome-wide copy number profiling:*
642 Embryos were collected immediately after 2 hours of egg laying. Salivary glands were dissected
643 in EBR from 50 wandering 3rd instar larvae per genotype and flash frozen. Ovaries were
644 dissected from females fattened for two days on wet yeast in EBR and 50 stage 13 egg
645 chambers were isolated for each genotype and flash frozen. Tissues were thawed on ice,
646 resuspended in LB3 and dounced using a Kontes B-type pestle. Dounced homogenates were
647 sonicated using a Bioruptor 300 (Diagenode) for 10 cycles of 30" on and 30'' off at maximal
648 power. Lysates were treated with RNase and Proteinase K and genomic DNA was isolated by
649 phenol-chloroform extraction. Illumina libraries were prepared using NEB DNA Ultra II (New
650 England Biolabs) following the manufacturers protocol. Barcoded libraries were sequenced
651 using Illumina NextSeq500 platform.
652
653 *Bioinformatics:*
654 Reads were mapped to the Drosophila genome (BDGP Release 6) using BWA using default
655 parameters (Li and Durbin, 2009). CNVnator 0.3.3 was used for the detection of
656 underreplicated regions using a bin size of 1000 (Abyzov et al., 2011). Regions were identified
657 as underreplicated if they were identified as underreplicated in 0-2h embryonic DNA and were

658 greater than 10kb in length. The number of reads for underreplicated regions was called by
659 using bedtools multicov tool for the underreplicated and uncalled regions. Average read depth
660 per region was determined by multiplying the number of reads in a region by the read length
661 and dividing by the total region length. Read depth was normalized between samples by scaling
662 the total reads obtained per sample. Statistical comparison between the regions was with a t-
663 test. For read depth in pericentric heterochromatin regions, the chromatin arm was binned into
664 10kb windows and the number of reads for each window was called using bedtools multicov
665 using only uniquely mapped reads.
666
667 Half maximum analysis of amplicon copy number profiles was performed as described
668 previously (Alexander et al., 2015; Nordman et al., 2014). Briefly, $\log_2$ ratios were generated
669 using bamCompare from deepTool 2.5.0 by comparing stage 13 follicle cell profiles to a 0-2h
670 embryo sample. Smoothed $\log_2$-transformed data was used to determine the point of
671 maximum copy number associated with each amplicon. The chromosome coordinate
672 corresponding to half the maximum value for each arm of the amplicon was then determined.
673
674 *Copy number analysis by droplet-digital PCR (ddPCR)*
675 Genomic DNA was extracted from salivary glands isolated from wandering 3rd instar larvae as
676 described above. Primer sets annealing to the mid-point of the indicated UR regions were used
677 (previously described in (Nordman et al., 2014; Sher et al., 2012)). ddPCR was performed
678 according to manufacture's recommendations (BioRad). All ddPCR reactions were performed in
679 triplicate from three independent biological replicates. The concentration value for each set of

680 primers in an underreplicated domain was divided by the concentration value of a fully
681 replicated control to generate the bar graph. Error bars represent the SEM.
682
683 *Western blotting:*
684 Ovaries were dissected from females fattened for two days on wet yeast and suspended in
685 Laemmli buffer supplemented with DTT. Ovaries were homogenized and boiled and extracts
686 were loaded on a 4-20% Mini-PROTEAN TGX Stain-Free gel (BioRad). After electrophoresis the
687 gel was activated and imaged according to the manufacturers recommendations. Protein was
688 transferred to a PDVF membrane using a Trans-Blot Turbo Transfer System (BioRad). After
689 blocking and incubation with antibodies, blots were imaged using an Amersham 600 CCD
690 imager.
691
692 **DATA ACCESS**
693 Data sets described in this manuscript can be found under the GEO accession number:
694 GSE114370.
695
696 **ACKNOWLEDGMENTS**
697 We thank Kristie Rose at the Vanderbilt Proteomics core for mass spectrometry and Olivia
698 Koues from the VANTAGE core at Vanderbilt for Illumina sequencing. Terry Orr-Weaver,
699 Stephen Bell, Katherine Friedman, James Dewar, Dave Cortez and members of the Nordman lab
700 for providing critical comments on the manuscript. We thank Brooke Hamilton for assistance in

generating the *Rif1* mutants. This work was supported by an NIH R00 award 5R00GM104151 to J.T.N.

DISCLOSURE

The authors have no conflicts of interest

REFERENCES

Abyzov, A., Urban, A.E., Snyder, M., Gerstein, M., 2011. CNVnator: an approach to discover, genotype, and characterize typical and atypical CNVs from family and population genome sequencing. Genome Res. 21, 974–984. doi:10.1101/gr.114876.110

Aggarwal, B.D., Calvi, B.R., 2004. Chromatin regulates origin activity in Drosophila follicle cells. Nature 430, 372–376. doi:10.1038/nature02694

Alabert, C., Bukowski-Wills, J.-C., Lee, S.-B., Kustatscher, G., Nakamura, K., de Lima Alves, F., Menard, P., Mejlvang, J., Rappsilber, J., Groth, A., 2014. Nascent chromatin capture proteomics determines chromatin dynamics during DNA replication and identifies unknown fork components. Nature Cell Biology 16, 281–293. doi:doi:10.1038/ncb2918

Alexander, J.L., Barrasa, M.I., Orr-Weaver, T.L., 2015. Replication fork progression during re-replication requires the DNA damage checkpoint and double-strand break repair. Curr. Biol. 25, 1654–1660. doi:10.1016/j.cub.2015.04.058

Alver, R.C., Chadha, G.S., Gillespie, P.J., Blow, J.J., 2017. Reversal of DDK-Mediated MCM Phosphorylation by Rif1-PP1 Regulates Replication Initiation and Replisome Stability Independently of ATR/Chk1. Cell Reports 18, 2508–2520. doi:10.1016/j.celrep.2017.02.042

Andreyeva, E.N., Bernardo, T.J., Kolesnikova, T.D., Lu, X., Yarinich, L.A., Bartholdy, B.A., Guo, X., Posukh, O.V., Healton, S., Willcockson, M.A., Pindyurin, A.V., Zhimulev, I.F., Skoultchi, A.I., Fyodorov, D.V., 2017. Regulatory functions and chromatin loading dynamics of linker histone H1 during endoreplication in Drosophila. Genes Dev. 31, 603–616. doi:10.1101/gad.295717.116

Andreyeva, E.N., Kolesnikova, T.D., Belyaeva, E.S., Glaser, R.L., Zhimulev, I.F., 2008. Local DNA underreplication correlates with accumulation of phosphorylated H2Av in the Drosophila

melanogaster polytene chromosomes. Chromosome Res. 16, 851–862. doi:10.1007/s10577-008-1244-4

Barolo, S., Carver, L.A., Posakony, J.W., 2000. GFP and beta-galactosidase transformation vectors for promoter/enhancer analysis in Drosophila. BioTechniques 29, 726, 728, 730, 732.

Bassett, A.R., Tibbit, C., Ponting, C.P., Liu, J.-L., 2013. Highly Efficient Targeted Mutagenesis of Drosophila with the CRISPR/Cas9 System. Cell Reports 1–9. doi:10.1016/j.celrep.2013.06.020

Beadle, G.W., Ephrussi, B., 1935. Transplantation in Drosophila. Proc. Natl. Acad. Sci. U.S.A. 21, 642–646.

Bell, S.P., Labib, K., 2016. Chromosome Duplication in Saccharomyces cerevisiae. Genetics 203, 1027–1067. doi:10.1534/genetics.115.186452

Belyaeva, E.S., Goncharov, F.P., Demakova, O.V., Kolesnikova, T.D., Boldyreva, L.V., Semeshin, V.F., Zhimulev, I.F., 2012. Late replication domains in polytene and non-polytene cells of Drosophila melanogaster. PLoS ONE 7, e30035. doi:10.1371/journal.pone.0030035

Blumenthal, A.B., Kriegstein, H.J., Hogness, D.S., 1974. The Units of DNA Replication in Drosophila melanogaster Chromosomes. Cold Spring Harb. Symp. Quant. Biol. 38, 205–223. doi:10.1101/SQB.1974.038.01.024

Calvi, B.R., Lilly, M.A., Spradling, A.C., 1998. Cell cycle control of chorion gene amplification. Genes Dev. 12, 734–744.

Cayrou, C., Coulombe, P., Vigneron, A., Stanojcic, S., Ganier, O., Peiffer, I., Rivals, E., Puy, A., Laurent-Chabalier, S., Desprat, R., Méchali, M., 2011. Genome-scale analysis of metazoan replication origins reveals their organization in specific but flexible sites defined by conserved features. Genome Res. 21, 1438–1449. doi:10.1101/gr.121830.111

Chapman, J.R., Barral, P., Vannier, J.B., Borel, V., Steger, M., 2013. RIF1 Is Essential for 53BP1-Dependent Nonhomologous End Joining and Suppression of DNA Double-Strand Break Resection. Molecular Cell. 49, 858-871

Claycomb, J.M., Macalpine, D.M., Evans, J.G., Bell, S.P., Orr-Weaver, T.L., 2002. Visualization of replication initiation and elongation in Drosophila. J. Cell Biol. 159, 225–236. doi:10.1083/jcb.200207046

Claycomb, J.M., Orr-Weaver, T.L., 2005. Developmental gene amplification: insights into DNA replication and gene expression. Trends Genet 21, 149–162. doi:10.1016/j.tig.2005.01.009

781 Cornacchia, D., Dileep, V., Quivy, J.-P., Foti, R., Tili, F., Mellwig, R.S., Antony, C., Almouzni, G.,
782 Gilbert, D.M., Buonomo, S.B.C., 2012. Mouse Rif1 is a key regulator of the replication-
783 timing programme in mammalian cells. EMBO J. 31, 3678–3690.
784 doi:10.1038/emboj.2012.214
785
786 Davé, A., Cooley, C., Garg, M., Bianchi, A., 2014. Protein phosphatase 1 recruitment by Rif1
787 regulates DNA replication origin firing by counteracting DDK activity. Cell Reports 7, 53–61.
788 doi:10.1016/j.celrep.2014.02.019
789
790 Debatisse, M., Le Tallec, B., Letessier, A., Dutrillaux, B., Brison, O., 2012. Common fragile sites:
791 mechanisms of instability revisited. Trends Genet 28, 22–32. doi:10.1016/j.tig.2011.10.003
792
793 Demakova, O.V., Pokholkova, G.V., Kolesnikova, T.D., Demakov, S.A., Andreyeva, E.N., Belyaeva,
794 E.S., Zhimulev, I.F., 2007. The SU(VAR)3-9/HP1 Complex Differentially Regulates the
795 Compaction State and Degree of Underreplication of X Chromosome Pericentric
796 Heterochromatin in Drosophila melanogaster. Genetics 175, 609–620.
797 doi:10.1534/genetics.106.062133
798
799 Di Virgilio, M., Callen, E., Yamane, A., Zhang, W., Jankovic, M., Gitlin, A.D., Feldhahn, N., Resch,
800 W., Oliveira, T.Y., Chait, B.T., Nussenzweig, A., Casellas, R., Robbiani, D.F., Nussenzweig,
801 M.C., 2013. Rif1 Prevents Resection of DNA Breaks and Promotes Immunoglobulin Class
802 Switching. Science 339, 711–715. doi:10.1128/MCB.22.2.555-566.2002
803
804 Durkin, S.G., Glover, T.W., 2007. Chromosome fragile sites. Annu. Rev. Genet. 41, 169–192.
805 doi:10.1146/annurev.genet.41.042007.165900
806
807 Eaton, M.L., Prinz, J.A., MacAlpine, H.K., Tretyakov, G., Kharchenko, P.V., Macalpine, D.M.,
808 2011. Chromatin signatures of the Drosophila replication program. Genome Res. 21, 164–
809 174. doi:10.1101/gr.116038.110
810
811 Edgar, B.A., Orr-Weaver, T.L., 2001. Endoreplication cell cycles: more for less. Cell 105, 297–
812 306.
813
814 Filion, G.J., van Bemmel, J.G., Braunschweig, U., Talhout, W., Kind, J., Ward, L.D., Brugman, W.,
815 de Castro, I.J., Kerkhoven, R.M., Bussemaker, H.J., van Steensel, B., 2010. Systematic
816 protein location mapping reveals five principal chromatin types in Drosophila cells. Cell 143,
817 212–224. doi:10.1016/j.cell.2010.09.009
818
819 Foti, R., Gnan, S., Cornacchia, D., Dileep, V., Bulut-Karslioglu, A., Diehl, S., Buness, A., Klein, F.A.,
820 Huber, W., Johnstone, E., Loos, R., Bertone, P., Gilbert, D.M., Manke, T., Jenuwein, T.,
821 Buonomo, S.C.B., 2015. Nuclear Architecture Organized by Rif1 Underpins the Replication-
822 Timing Program. Molecular Cell. doi:10.1016/j.molcel.2015.12.001
823
824 Gilbert, D.M., 2002. Replication timing and transcriptional control: beyond cause and effect.

825 Curr. Opin. Cell Biol. 14, 377–383.
826
827 Gratz, S.J., Cummings, A.M., Nguyen, J.N., Hamm, D.C., Donohue, L.K., Harrison, M.M.,
828 Wildonger, J., O'Connor-Giles, K.M., 2013. Genome Engineering of Drosophila with the
829 CRISPR RNA-Guided Cas9 Nuclease. Genetics. doi:10.1534/genetics.113.152710
830
831 Gratz, S.J., Rubinstein, C.D., Harrison, M.M., Wildonger, J., O'Connor-Giles, K.M., 2015. CRISPR-
832 Cas9 Genome Editing in Drosophila. Curr Protoc Mol Biol 111, 31.2.1–31.2.20.
833 doi:10.1002/0471142727.mb3102s111
834
835 Hannibal, R.L., Baker, J.C., 2016. Selective Amplification of the Genome Surrounding Key
836 Placental Genes in Trophoblast Giant Cells. Current Biology 1–18.
837 doi:10.1016/j.cub.2015.11.060
838
839 Hannibal, R.L., Chuong, E.B., Rivera-Mulia, J.C., Gilbert, D.M., Valouev, A., Baker, J.C., 2014.
840 Copy Number Variation Is a Fundamental Aspect of the Placental Genome. PLoS Genet. 10,
841 e1004290. doi:10.1371/journal.pgen.1004290
842
843 Hardy, C.F., Sussel, L., Shore, D., 1992. A RAP1-interacting protein involved in transcriptional
844 silencing and telomere length regulation. Genes & Dev 6, 801–814.
845 doi:10.1101/gad.6.5.801
846
847 Hayano, M., Kanoh, Y., Matsumoto, S., Renard-Guillet, C., Shirahige, K., Masai, H., 2012. Rif1 is a
848 global regulator of timing of replication origin firing in fission yeast. Genes & Dev 26, 137–
849 150. doi:10.1101/gad.178491.111
850
851 Hiraga, S.-I., Alvino, G.M., Chang, F., Lian, H.-Y., Sridhar, A., Kubota, T., Brewer, B.J., Weinreich,
852 M., Raghuraman, M.K., Donaldson, A.D., 2014. Rif1 controls DNA replication by directing
853 Protein Phosphatase 1 to reverse Cdc7-mediated phosphorylation of the MCM complex.
854 Genes Dev. 28, 372–383. doi:10.1101/gad.231258.113
855
856 Hiraga, S.-I., Ly, T., Garzón, J., Hořejší, Z., Ohkubo, Y.N., Endo, A., Obuse, C., Boulton, S.J.,
857 Lamond, A.I., Donaldson, A.D., 2017. Human RIF1 and protein phosphatase 1 stimulate DNA
858 replication origin licensing but suppress origin activation. EMBO Rep. 18, 403–419.
859 doi:10.15252/embr.201641983
860
861 Hua, B.L., Orr-Weaver, T.L., 2017. DNA Replication Control During Drosophila Development:
862 Insights into the Onset of S Phase, Replication Initiation, and Fork Progression. Genetics
863 207, 29–47. doi:10.1534/genetics.115.186627
864
865 Jackson, A.P., Laskey, R.A., Coleman, N., 2014. Replication proteins and human disease. Cold
866 Spring Harbor Perspectives in Biology 6. doi:10.1101/cshperspect.a013060
867
868 Kolesnikova, T.D., Makunin, I.V., Volkova, E.I., Pirrotta, V., Belyaeva, E.S., Zhimulev, I.F., 2005.

869 Functional dissection of the Suppressor of UnderReplication protein of Drosophila
870 melanogaster: identification of domains influencing chromosome binding and DNA
871 replication. Genetica 124, 187–200.
872
873 Kolesnikova, T.D., Posukh, O.V., Andreyeva, E.N., Bebyakina, D.S., Ivankin, A.V., Zhimulev, I.F.,
874 2013. Drosophila SUUR protein associates with PCNA and binds chromatin in a cell cycle-
875 dependent manner. Chromosoma 122, 55–66. doi:10.1007/s00412-012-0390-9
876
877 Letessier, A., Millot, G.A., Koundrioukoff, S., Lachagès, A.-M., Vogt, N., Hansen, R.S., Malfoy, B.,
878 Brison, O., Debatisse, M., 2011. Cell-type-specific replication initiation programs set fragility
879 of the FRA3B fragile site. Nature 470, 120–123. doi:10.1038/nature09745
880
881 Li, H., Durbin, R., 2009. Fast and accurate short read alignment with Burrows-Wheeler
882 transform. Bioinformatics 25, 1754–1760. doi:10.1093/bioinformatics/btp324
883
884 Lifeng Xu, E.H.B., 2004. Human Rif1 protein binds aberrant telomeres and aligns along anaphase
885 midzone microtubules. J. Cell Biol. 167, 819–830. doi:10.1083/jcb.200408181
886
887 Lilly, M.A., Duronio, R.J., 2005. New insights into cell cycle control from the Drosophila
888 endocycle. Oncogene 24, 2765–2775. doi:10.1038/sj.onc.1208610
889
890 MacAlpine, H.K., Gordân, R., Powell, S.K., Hartemink, A.J., Macalpine, D.M., 2010. Drosophila
891 ORC localizes to open chromatin and marks sites of cohesin complex loading. Genome Res.
892 20, 201–211. doi:10.1101/gr.097873.109
893
894 Makunin, I.V., Volkova, E.I., Belyaeva, E.S., Nabirochkina, E.N., Pirrotta, V., Zhimulev, I.F., 2002.
895 The Drosophila suppressor of underreplication protein binds to late-replicating regions of
896 polytene chromosomes. Genetics 160, 1023–1034.
897
898 Matson, J.P., Dumitru, R., Coryell, P., Baxley, R.M., Chen, W., Twaroski, K., Webber, B.R., Tolar,
899 J., Bielinsky, A.-K., Purvis, J.E., Cook, J.G., 2017. Rapid DNA replication origin licensing
900 protects stem cell pluripotency. Elife 6. doi:10.7554/eLife.30473
901
902 Mattarocci, S., Shyian, M., Lemmens, L., Damay, P., Altintas, D.M., Shi, T., Bartholomew, C.R.,
903 Thomä, N.H., Hardy, C.F.J., Shore, D., 2014. Rif1 controls DNA replication timing in yeast
904 through the PP1 phosphatase Glc7. Cell Reports 7, 62–69. doi:10.1016/j.celrep.2014.03.010
905
906 Mesner, L.D., Valsakumar, V., Karnani, N., Dutta, A., Hamlin, J.L., Bekiranov, S., 2011. Bubble-
907 chip analysis of human origin distributions demonstrates on a genomic scale significant
908 clustering into zones and significant association with transcription. Genome Res. 21, 377–
909 389. doi:10.1101/gr.111328.110
910
911 Miotto, B., Ji, Z., Struhl, K., 2016. Selectivity of ORC binding sites and the relation to replication
912 timing, fragile sites, and deletions in cancers. Proc. Natl. Acad. Sci. U.S.A. 113, E4810–

913 E4819. doi:10.1073/pnas.1609060113
914
915 Moore, D.P., Orr-Weaver, T.L., 1998. Chromosome segregation during meiosis: building an
916 unambivalent bivalent. Curr Top Dev Biol 37, 263–299.
917
918 Newman, T.J., Mamun, M.A., Nieduszynski, C.A., Blow, J.J., 2013. Replisome stall events have
919 shaped the distribution of replication origins in the genomes of yeasts. Nucleic Acids Res.
920 doi:10.1093/nar/gkt728
921
922 Nordman, J., Li, S., Eng, T., Macalpine, D., Orr-Weaver, T.L., 2011. Developmental control of the
923 DNA replication and transcription programs. Genome Res. 21, 175–181.
924 doi:10.1101/gr.114611.110
925
926 Nordman, J.T., Kozhevnikova, E.N., Verrijzer, C.P., Pindyurin, A.V., Andreyeva, E.N., Shloma,
927 V.V., Zhimulev, I.F., Orr-Weaver, T.L., 2014. DNA Copy-Number Control through Inhibition
928 of Replication Fork Progression. Cell Reports 9, 841–849. doi:10.1016/j.celrep.2014.10.005
929
930 Nordman, J.T., Orr-Weaver, T.L., 2015. Understanding replication fork progression, stability, and
931 chromosome fragility by exploiting the Suppressor of Underreplication protein. Bioessays.
932 doi:10.1002/bies.201500021
933
934 Norio, P., Kosiyatrakul, S., Yang, Q., Guan, Z., Brown, N.M., Thomas, S., Riblet, R., Schildkraut,
935 C.L., 2005. Progressive activation of DNA replication initiation in large domains of the
936 immunoglobulin heavy chain locus during B cell development. Mol. Cell 20, 575–587.
937 doi:10.1016/j.molcel.2005.10.029
938
939 Peace, J.M., Ter-Zakarian, A., Aparicio, O.M., 2014. Rif1 Regulates Initiation Timing of Late
940 Replication Origins throughout the *S. cerevisiae* Genome. PLoS ONE 9, e98501.
941 doi:10.1371/journal.pone.0098501
942
943 Pindyurin, A.V., Boldyreva, L.V., Shloma, V.V., Kolesnikova, T.D., Pokholkova, G.V., Andreyeva,
944 E.N., Kozhevnikova, E.N., Ivanoschuk, I.G., Zarutskaya, E.A., Demakov, S.A., Gorchakov, A.A.,
945 Belyaeva, E.S., Zhimulev, I.F., 2008. Interaction between the Drosophila heterochromatin
946 proteins SUUR and HP1. J. Cell. Sci. 121, 1693–1703. doi:10.1242/jcs.018655
947
948 Pindyurin, A.V., Moorman, C., de Wit, E., Belyakin, S.N., Belyaeva, E.S., Christophides, G.K.,
949 Kafatos, F.C., van Steensel, B., Zhimulev, I.F., 2007. SUUR joins separate subsets of PcG, HP1
950 and B-type lamin targets in Drosophila. J. Cell. Sci. 120, 2344–2351. doi:10.1242/jcs.006007
951
952
953 Remus, D., Beall, E.L., Botchan, M.R., 2004. DNA topology, not DNA sequence, is a critical
954 determinant for Drosophila ORC-DNA binding. EMBO J. 23, 897–907.
955 doi:10.1038/sj.emboj.7600077
956

957 Rhind, N., Gilbert, D.M., 2013. DNA replication timing. Cold Spring Harbor Perspectives in
958 Biology 5, a010132. doi:10.1101/cshperspect.a010132
959
960 Rudkin, G.T. 1969. Non replicating DNA in Drosophila. Genetics 61, 227-238.
961
962 Shao, Z., Raible, F., Mollaaghababa, R., Guyon, J.R., Wu, C.T., Bender, W., Kingston, R.E., 1999.
963 Stabilization of chromatin structure by PRC1, a Polycomb complex. Cell 98, 37–46.
964 doi:10.1016/S0092-8674(00)80604-2
965
966 Sharan, S.K., Thomason, L.C., Kuznetsov, S.G., Court, D.L., 2009. Recombineering: a homologous
967 recombination-based method of genetic engineering. Nat Protoc 4, 206–223.
968 doi:10.1038/nprot.2008.227
969
970 Sher, N., Bell, G.W., Li, S., Nordman, J., Eng, T., Eaton, M.L., Macalpine, D.M., Orr-Weaver, T.L.,
971 2012. Developmental control of gene copy number by repression of replication initiation
972 and fork progression. Genome Res. 22, 64–75. doi:10.1101/gr.126003.111
973
974 Siddiqui, K., On, K.F., Diffley, J.F.X., 2013. Regulating DNA replication in eukarya. Cold Spring
975 Harbor Perspectives in Biology 5. doi:10.1101/cshperspect.a012930
976
977 Spradling, A., Orr-Weaver, T., 1987. Regulation of DNA replication during Drosophila
978 development. Annu. Rev. Genet. 21, 373–403. doi:10.1146/annurev.ge.21.120187.002105
979
980 Sreesankar, E., Bharathi, V., Mishra, R.K., Mishra, K., 2015. Drosophila Rif1 is an essential gene
981 and controls late developmental events by direct interaction with PP1-87B. Sci Rep 5,
982 10679. doi:10.1038/srep10679
983
984 Sreesankar, E., Senthilkumar, R., Bharathi, V., Mishra, R.K., Mishra, K., 2012. Functional
985 diversification of yeast telomere associated protein, Rif1, in higher eukaryotes. BMC
986 Genomics 13, 255. doi:10.1186/1471-2164-13-255
987
988 Sukackaite, R., Cornacchia, D., Jensen, M.R., Mas, P.J., Blackledge, M., Enervald, E., Duan, G.,
989 Auchynnikava, T., Köhn, M., Hart, D.J., Buonomo, S.B.C., 2017. Mouse Rif1 is a regulatory
990 subunit of protein phosphatase 1 (PP1). Sci Rep 7, 2119. doi:10.1038/s41598-017-01910-1
991
992 Swenson, J.M., Colmenares, S.U., Strom, A.R., Costes, S.V., Karpen, G.H., 2016. The composition
993 and organization of Drosophila heterochromatin are heterogeneous and dynamic. Elife 5.
994 doi:10.7554/eLife.16096
995
996 Yamazaki, S., Ishii, A., Kanoh, Y., Oda, M., Nishito, Y., Masai, H., 2012. Rif1 regulates the
997 replication timing domains on the human genome. EMBO J. 31, 3667–3677.
998 doi:10.1038/emboj.2012.180
999
1000 Yarosh, W., Spradling, A.C., 2014. Incomplete replication generates somatic DNA alterations

within Drosophila polytene salivary gland cells. Genes Dev. 28, 1840–1855. doi:10.1101/gad.245811.114

Zielke, N., Edgar, B.A., DePamphilis, M.L., 2013. Endoreplication. Cold Spring Harbor Perspectives in Biology 5, a012948–a012948. doi:10.1101/cshperspect.a012948

Zimmermann, M., Lottersberger, F., Buonomo, S.B., Sfeir, A., de Lange, T., 2013. 53BP1 Regulates DSB Repair Using Rif1 to Control 5' End Resection. Science 339, 700–704. doi:10.1016/j.jsb.2005.06.002

FIGURE LEGENDS

Figure 1. The SNF2 domain is essential for SUUR function and replication fork localization.

(A) Schematic representation of the SUUR and SUUR$^{\Delta SNF}$ proteins. (B) Illumina-based copy number profiles (Reads Per Million; RPM) of *chr2L* 1-20,000,000 from larval salivary glands. Black bars below each profile represent underreplicated regions identified by CNVnator. (C) Average read depth in regions of euchromatic underreplication domains called in wild-type salivary glands vs. the full replicated regions of the genome. A Welch Two Sample t-test was used to determine *p* values. (D) Quantitative droplet-digital PCR (ddPCR) copy number assay for multiple underreplicated regions. Each bar is the average enrichment relative to fully replicated control region for three biological replicates. Error bars are the SEM. (E) Localization of SUUR in wild-type and *SuUR*$^{\Delta SNF}$ mutant follicle cells. A single representative stage 13 follicle cell nucleus is shown. Arrowheads indicate sites of amplification. Asterisk marks the chromocenter (heterochromatin). Scale bars are 2µm. DAPI=blue, SUUR=green, EdU=red.

Figure 2. Rif1 is required for underreplication.

(A) Schematic representation of the *Rif1* gene and CRISPR-induced *Rif1* mutants. Lightning bolts represent the 5' and 3' gRNA positions. (B) Illumina-based copy number profiles of the *chr2L* from larval salivary glands. Black bars below each profile represent underreplicated regions identified by CNVnator. The wild-type and *SuUR* profiles are the same as in Figure 1b. (C) Average read depth in regions of euchromatic underreplication domains called in wild-type salivary glands vs. the fully replicated regions of the genome. A Welch Two Sample t-test was used to determine *p* values. (D) Quantitative droplet-digital PCR (ddPCR) copy number assay for multiple underreplicated regions. Each bar is the average enrichment relative to fully replicated control region for three biological replicates. Error bars are the SEM.

Figure 3. Rif1 regulates replication fork progression.

(A) Illumina-based copy number profile of sites of follicle cell gene amplification. DNA was extracted from wild type and *Rif1* mutant stage 13 egg chambers and compared to DNA extracted from 0-2 hr embryos. The resulting graphs are the $\log_2$-transformed ratios of egg chamber relative to embryonic DNA. Bars below the graphs represent the distance between the half-maximum copy number on each side of the replication origin. (B) Fraction of cells that display visible amplification foci in each stage of gene amplification. Average of two biological replicates in which two egg chambers from each stage were used per biological replicate. 100-300 follicle cells were counted per genotype. Error bars are the SEM.

Figure 4. Rif1 acts downstream of SUUR.

1049 Localization of replication forks (EdU) and SUUR in a wild-type and *Rif1* mutant follicle cell
1050 nuclei. A single representative stage 13 follicle cell nucleus is shown. Scale bars are 2µm.
1051 Arrowheads indicate sites of amplification. Asterisks marks the chromocenter
1052 (heterochromatin). DAPI=blue, SUUR=green, EdU=red.
1053
1054
1055 **Figure 5. SUUR is necessary to retain Rif1 at replication forks.**
1056 Localization of active replication forks (EdU) and Rif1 in a wild-type and *SuUR* mutant follicle cell
1057 nuclei. Single representative follicle cell nuclei are shown for each stage. Scale bars are 2µm.
1058 Arrowheads indicate sites of amplification. Asterisk marks the chromocenter
1059 (heterochromatin).
1060
1061
1062 **Figure 6. The Rif1/PP1 interaction is necessary to promote underreplication.**
1063 (A) Quantitative droplet-digital PCR (ddPCR) copy number assay for multiple underreplicated
1064 regions. Each bar is the average enrichment relative to fully replicated control region for three
1065 biological replicates. Error bars are the SEM. (B) A new model for SUUR-mediated
1066 underreplication. In this model SUUR serves as a scaffold to recruit a Rif1/PP1 complex to
1067 replication forks where Rif1/PP1 inhibits replication fork progression through
1068 dephosphorylation of a component of the replisome. Replication fork image is adapted from
1069 (Nordman and Orr-Weaver, 2015)
1070

Supplemental Figure S1 – related to Figure 1. Genome-wide copy number profile of the *SuUR*$^{\Delta SNF}$ mutant.

Illumina-based copy number profiles of all chromosome arms except the fourth for larval salivary glands of the indicated genotypes and wild type 0-2h embryos in which DNA is fully replicated. Black bars below each profile represent called underreplicated regions.

Supplemental Figure S2 – related to Figure 2 and Figure 5. Verification of *Rif1* mutants and validation of anti-Rif1 antibody.

(A) Western blot analysis of ovary extracts prepared from the indicated genotypes. Serum produced in guinea pigs was used at 1:1000 dilution. (B) Immunofluorescence of ovaries using affinity purified anti-Rif1 antibody produced in guinea pigs. Exposure times were equal between the two genotypes. (C) Embryo hatch rate assay comparing embryos laid by wild-type or *Rif1*^{1}*/Rif1*^{2} mutant mothers. n=300 embryos per genotype. Each data point represents the hatch rate of a group of 10 embryos. An unpaired student t-test was used to generate the *p* value.

Supplemental Figure S3 – related to Figure 2. Genome-wide copy number profile of the *Rif1* mutant.

(A) Illumina-based copy number profiles of all chromosome arms except the fourth for larval salivary glands of the indicated genotypes. Black bars below each profile represent called underreplicated regions. (B) Box plot represents read depth in 10 kb bins in the pericentric chromatin regions for *chr 2L, 2R, 3L* and *3R*. A Welch Two Sample t-test was used to compare

1093 the same regions between *SuUR* and *Rif1* mutants. The same wild-type, *SuUR* and 0-2h embryo
1094 plots as in Supplemental Figure S1.
1095
1096 **Supplemental Figure S4. Rif1 mutant salivary gland cells display a pattern of late replication.**
1097 (A) Representative immunofluorescent images of 3rd instar salivary glands pulse labelled with
1098 EdU and stained with anti-HP1 to mark heterochromatin. Wild-type cells fail to incorporate EdU
1099 into regions of heterochromatin due to underreplication, whereas EdU can be detected in the
1100 heterochromatic regions of *SuUR* and *Rif1* mutants. DAPI=blue, EdU=green, HP1=red (B)
1101 Quantitation of three biological replicates. Out of the total number of EdU positive cells, the
1102 fraction incorporating EdU predominantly in the heterochromatic (HP1) regions were
1103 measured. More than 200 EdU positive cells were scored for each genotype.
1104
1105 **Supplemental Figure S5. *Rif1* mutant endo cycling cells have enlarged chromocenters.**
1106 Representative image of of nurse cell nuclei from stage 10 egg chambers. Egg chambers were
1107 stained with DAPI. Scale bar is 10 µm. Exposure times and scaling are equal in all images.
1108
1109 **Supplemental Figure S6 – related to Figure 6. The Rif1^{PP1} protein expression is similar to wild**
1110 **type Rif1.**
1111 (A) Western blot analysis of ovary extracts from *Rif1^{PP1}/Rif1^{1}* and *Rif1^{1}/+* adults. Serum was
1112 produced in guinea pigs and used at 1:1000 dilution.

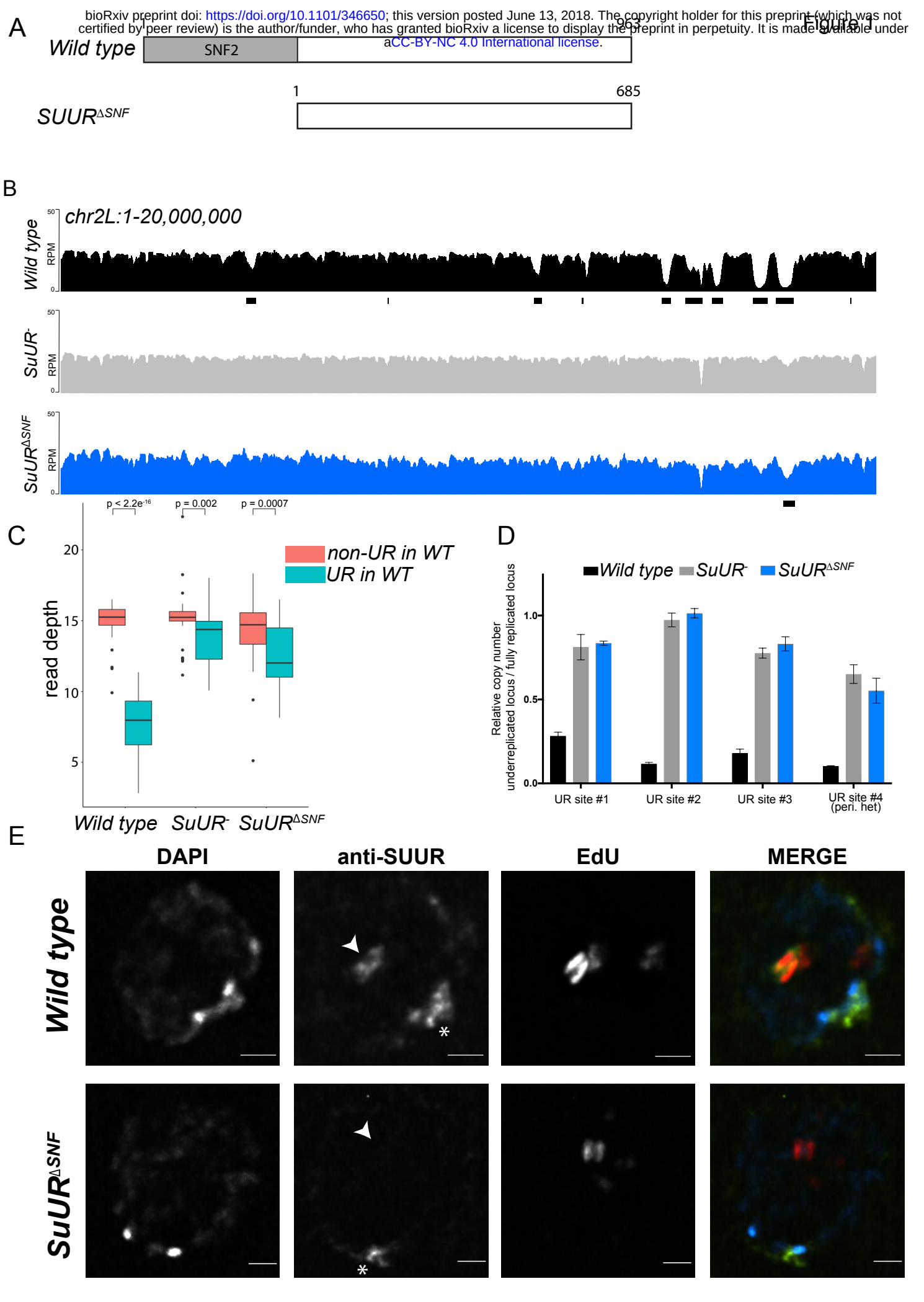

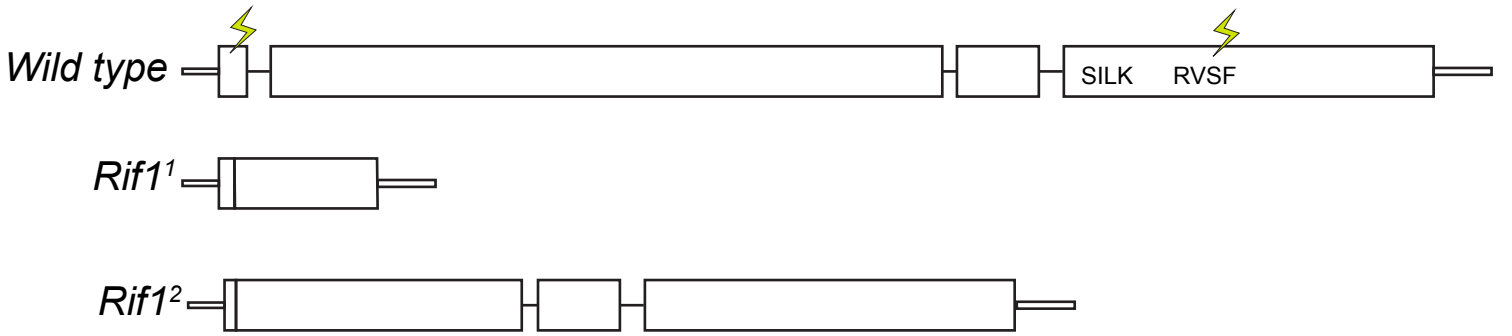

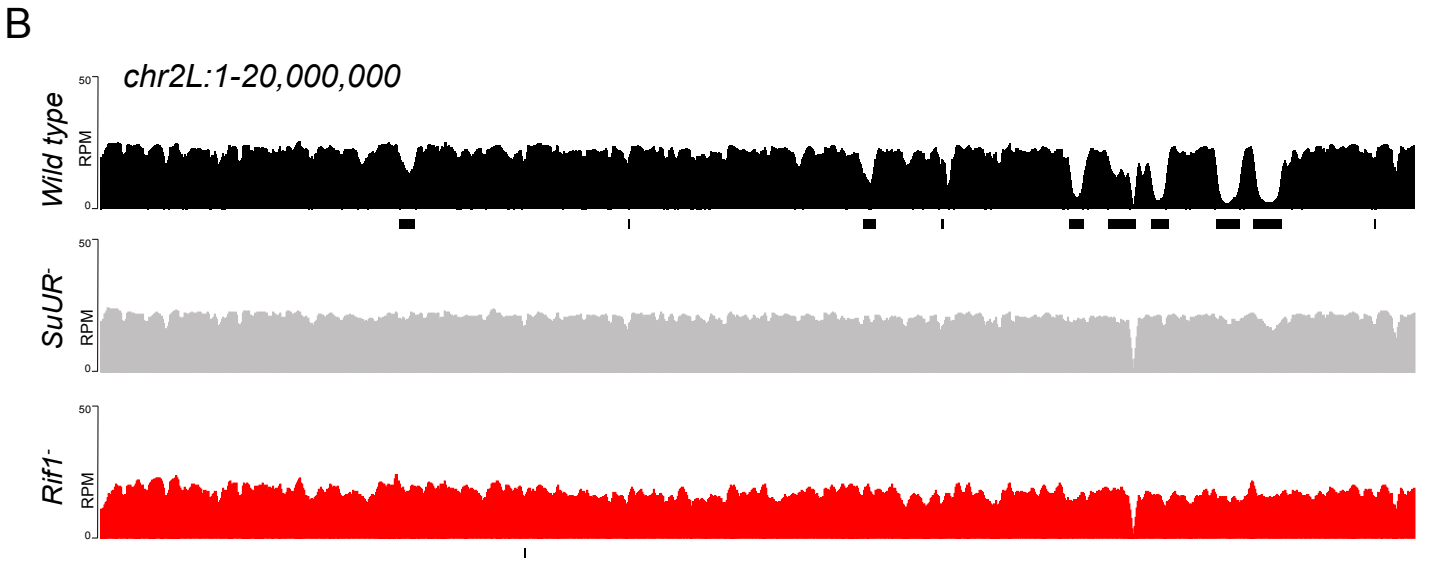

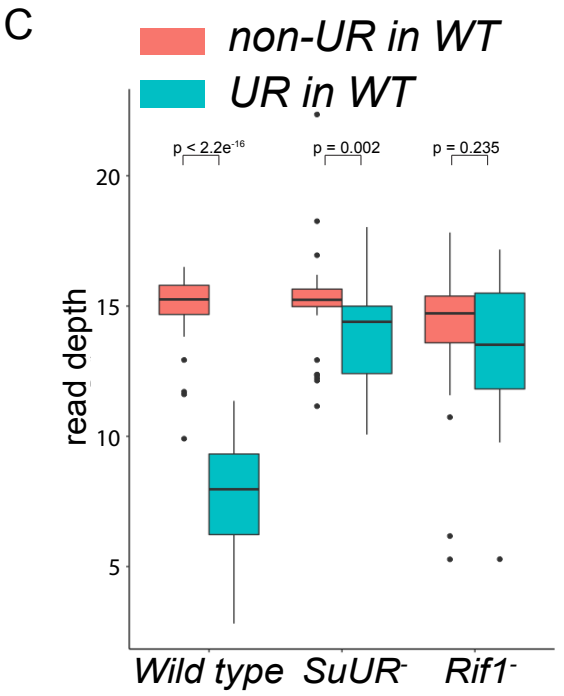

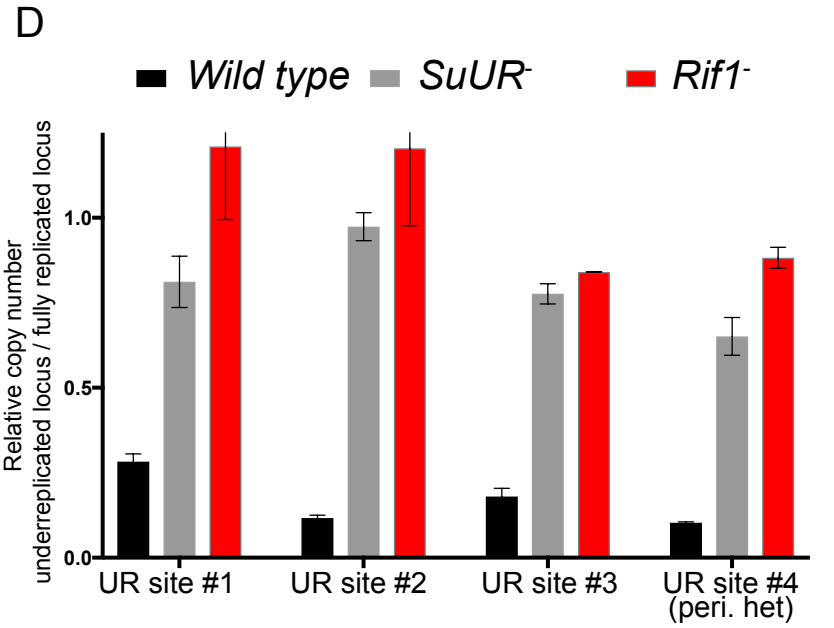

A

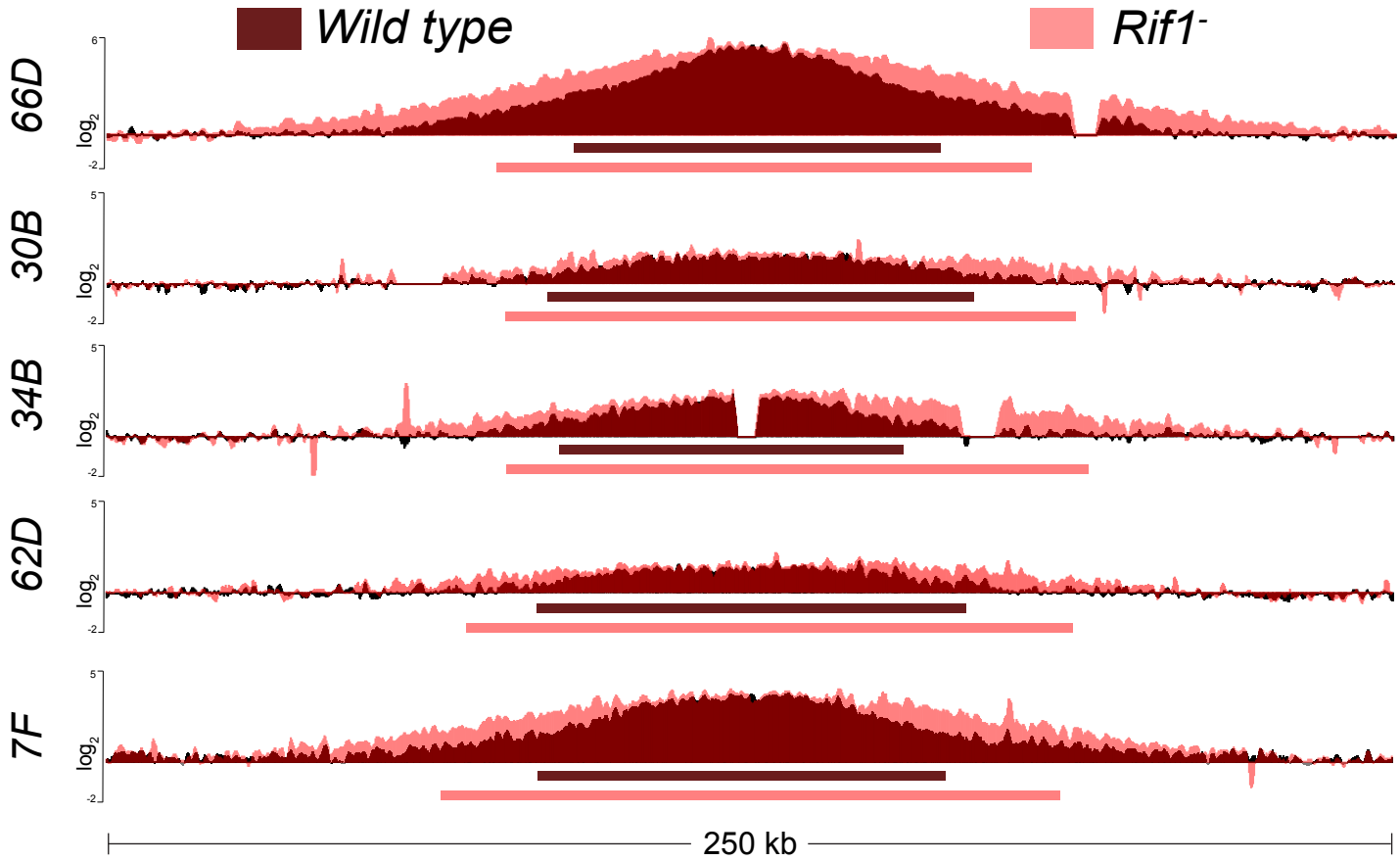

B

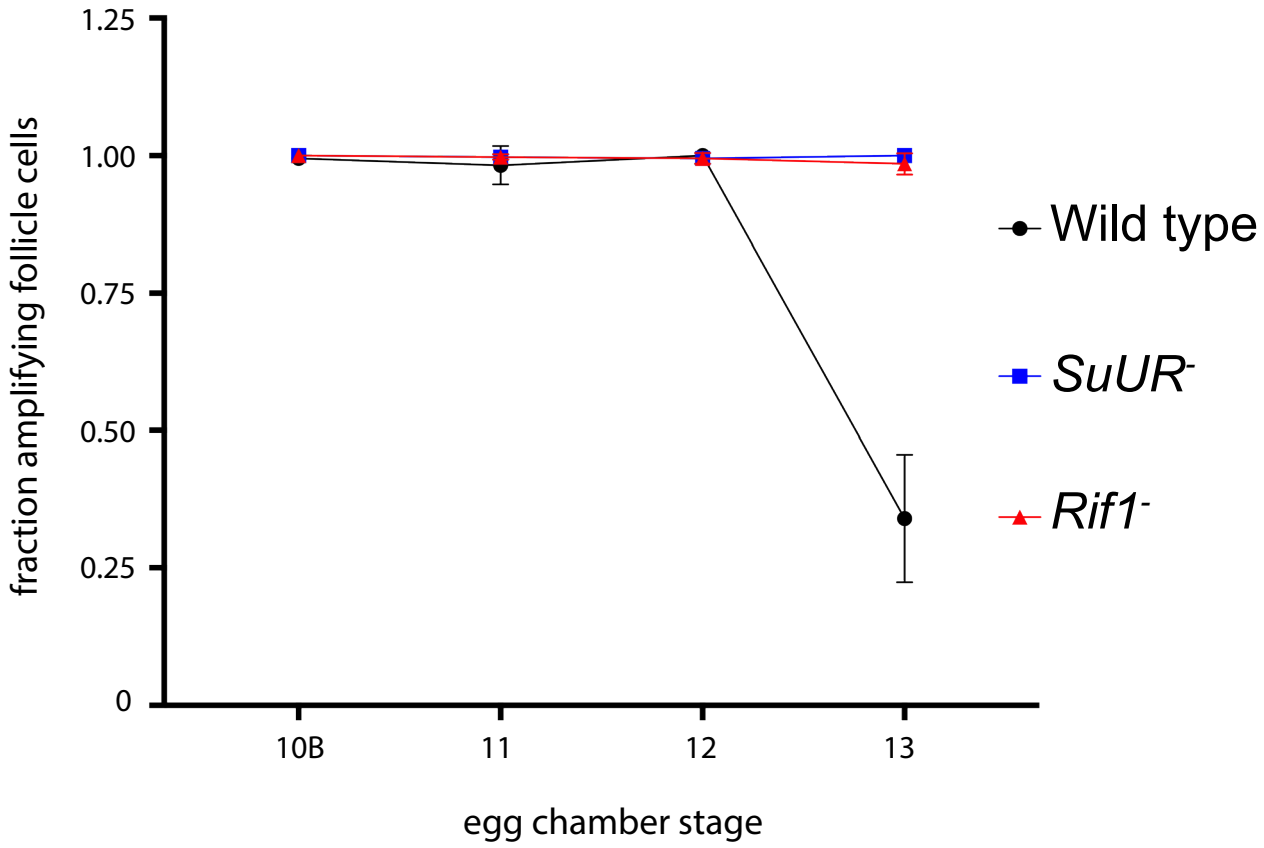

Figure 4

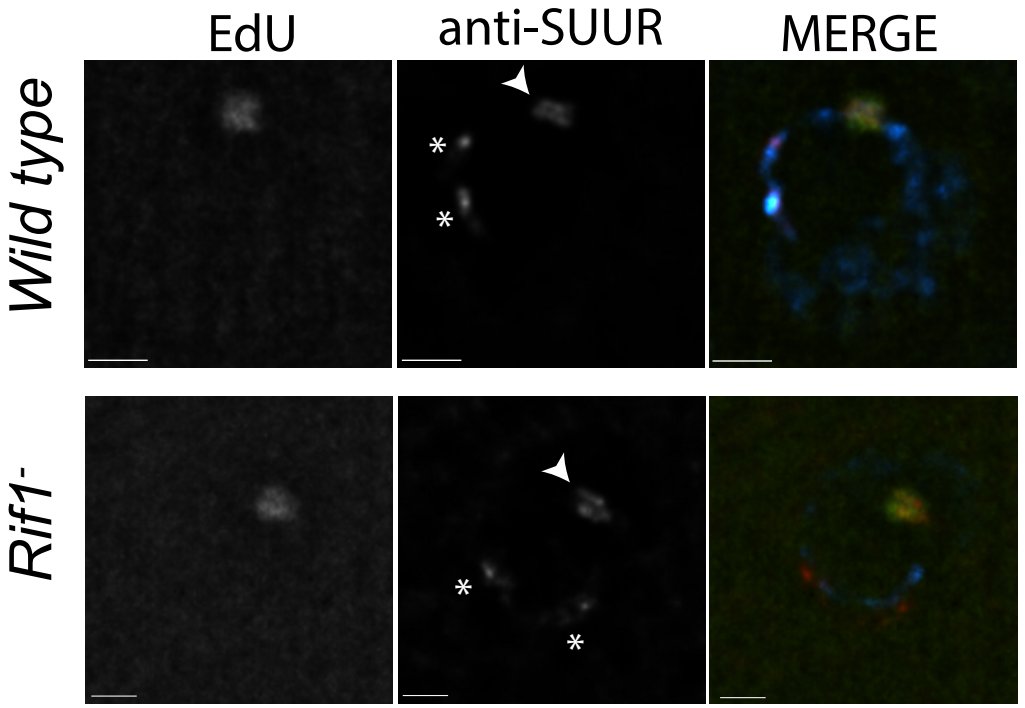

Figure 5

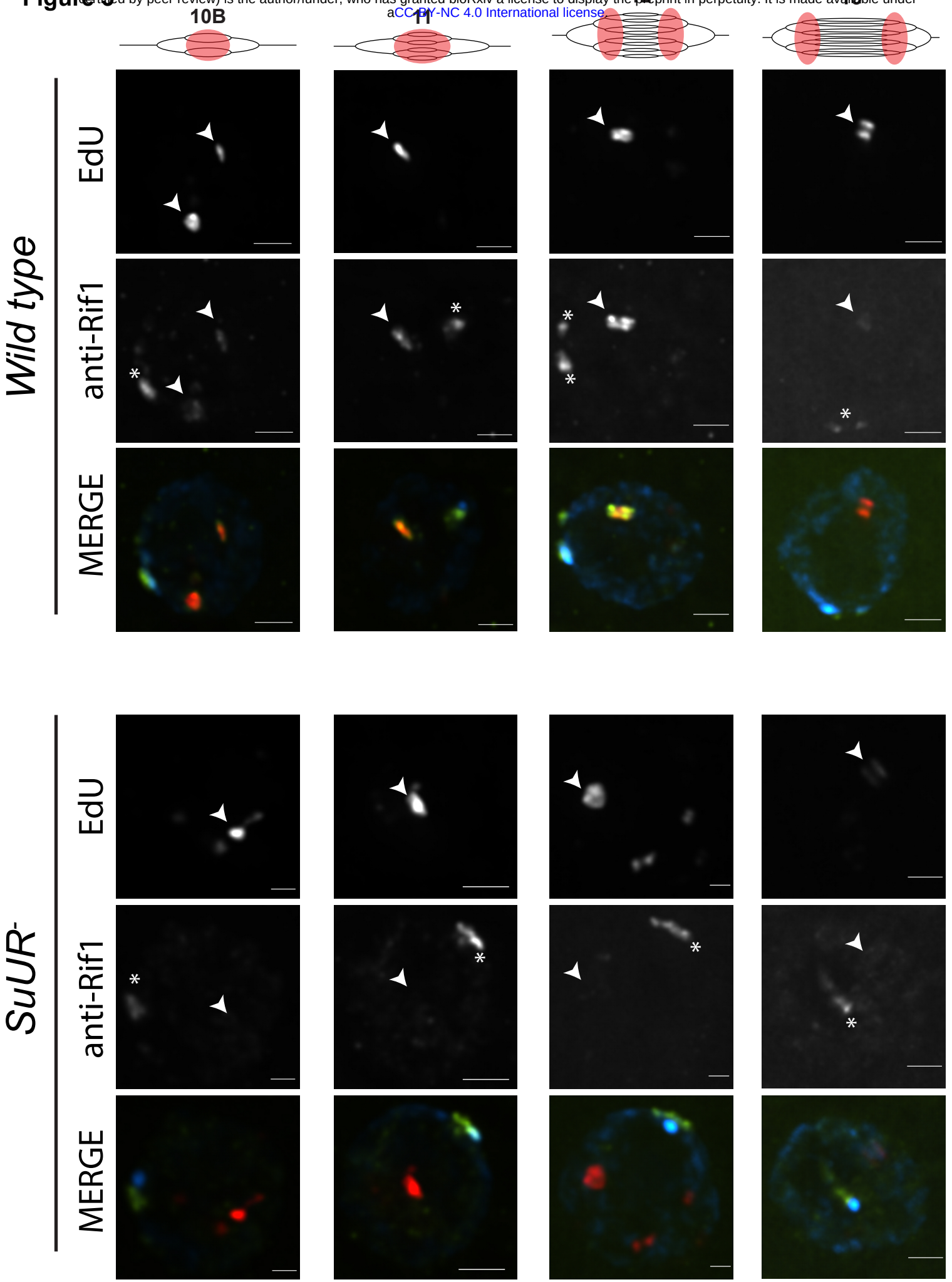

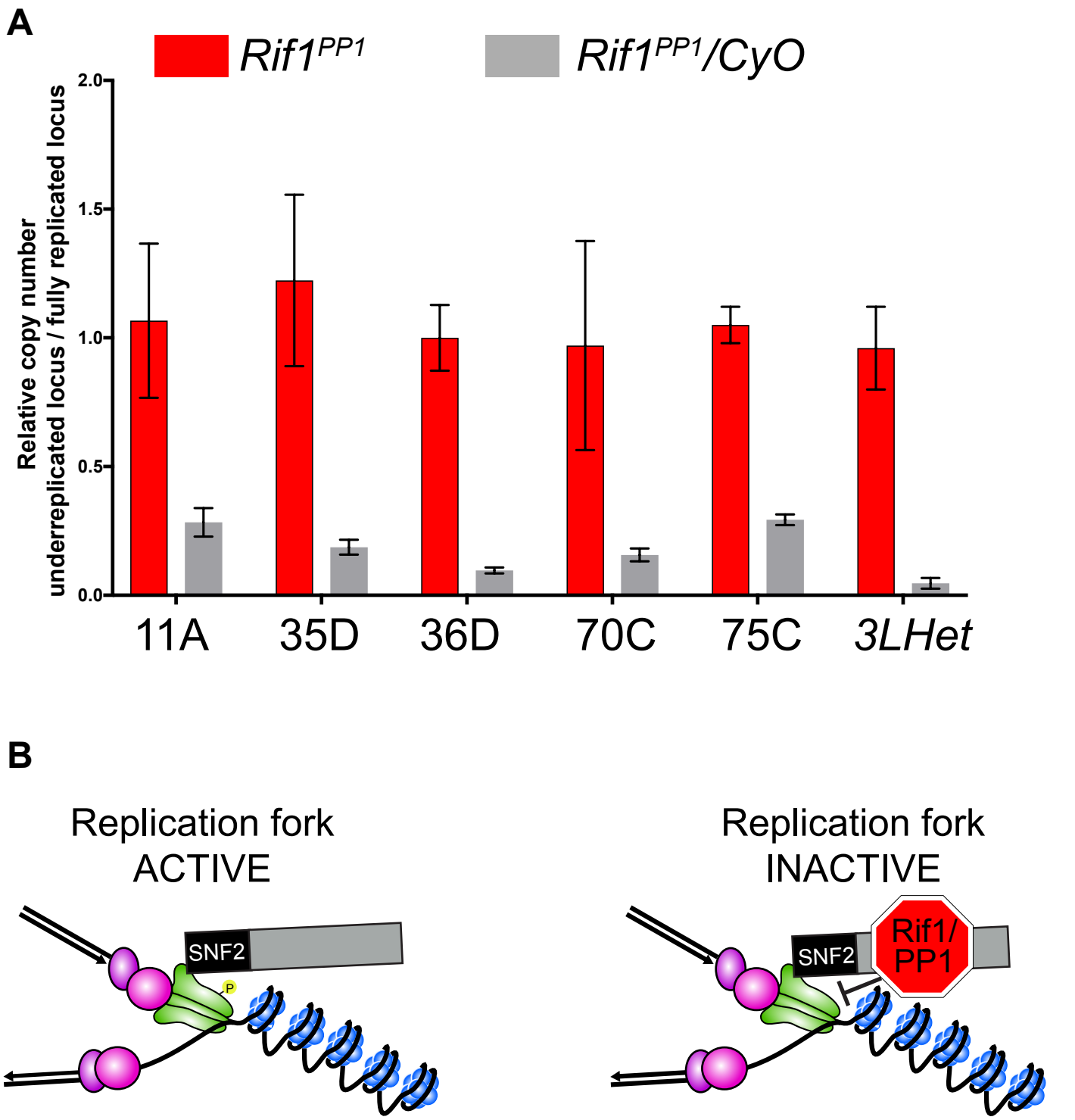

Table 1	Full length SUUR			SNF2 domain			negative control		
	Repl. #1	Repl. #2	Repl. #3	Repl. #1	Repl. #2	Repl. #3	Repl. #1	Repl. #2	Repl. #3
SUUR	36	48	26	21	18	10	1	1	2
Rif1(CG30085)	29	24	14	1	0	0	0	0	0

Comparison of Rif1 abundance*	
Full length vs. SNF2	$p < 0.00010$
Full length vs. neg. ctrl	$p < 0.00010$

*Fisher's Exact Test

Supplementary Figure 1

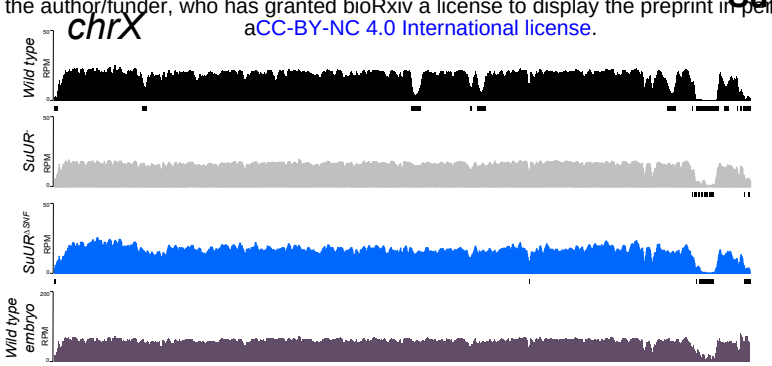

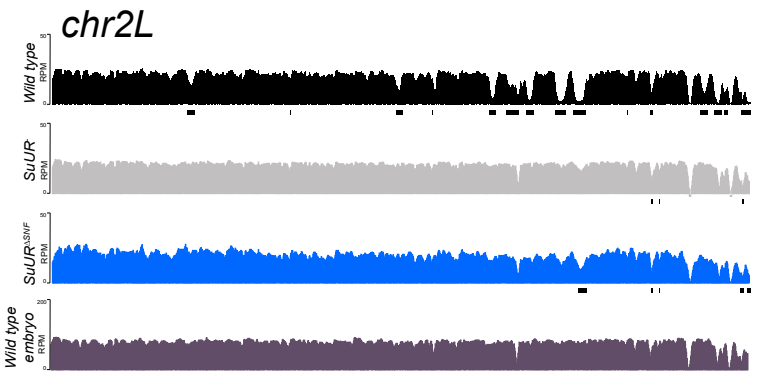

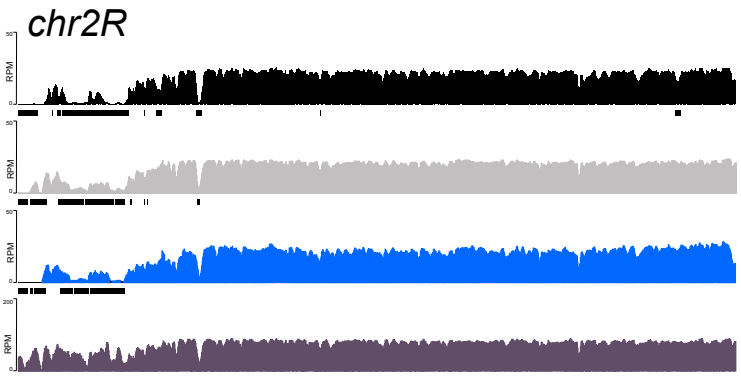

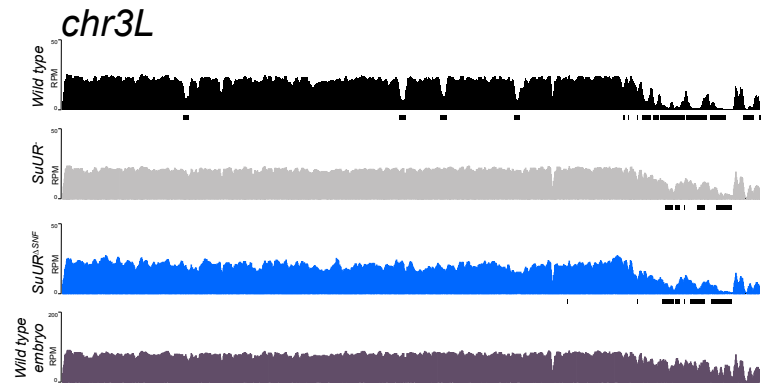

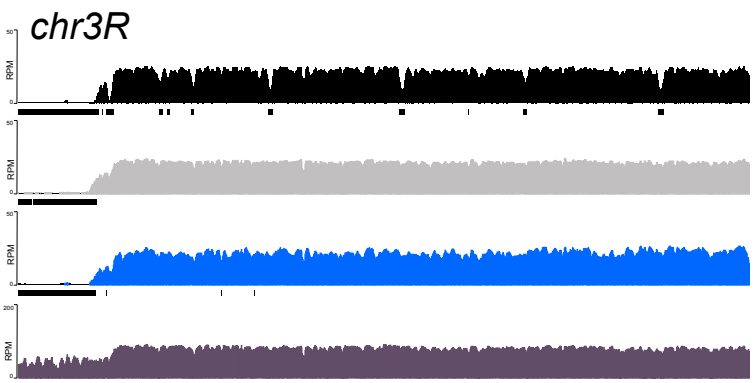

Supplementary Figure 2

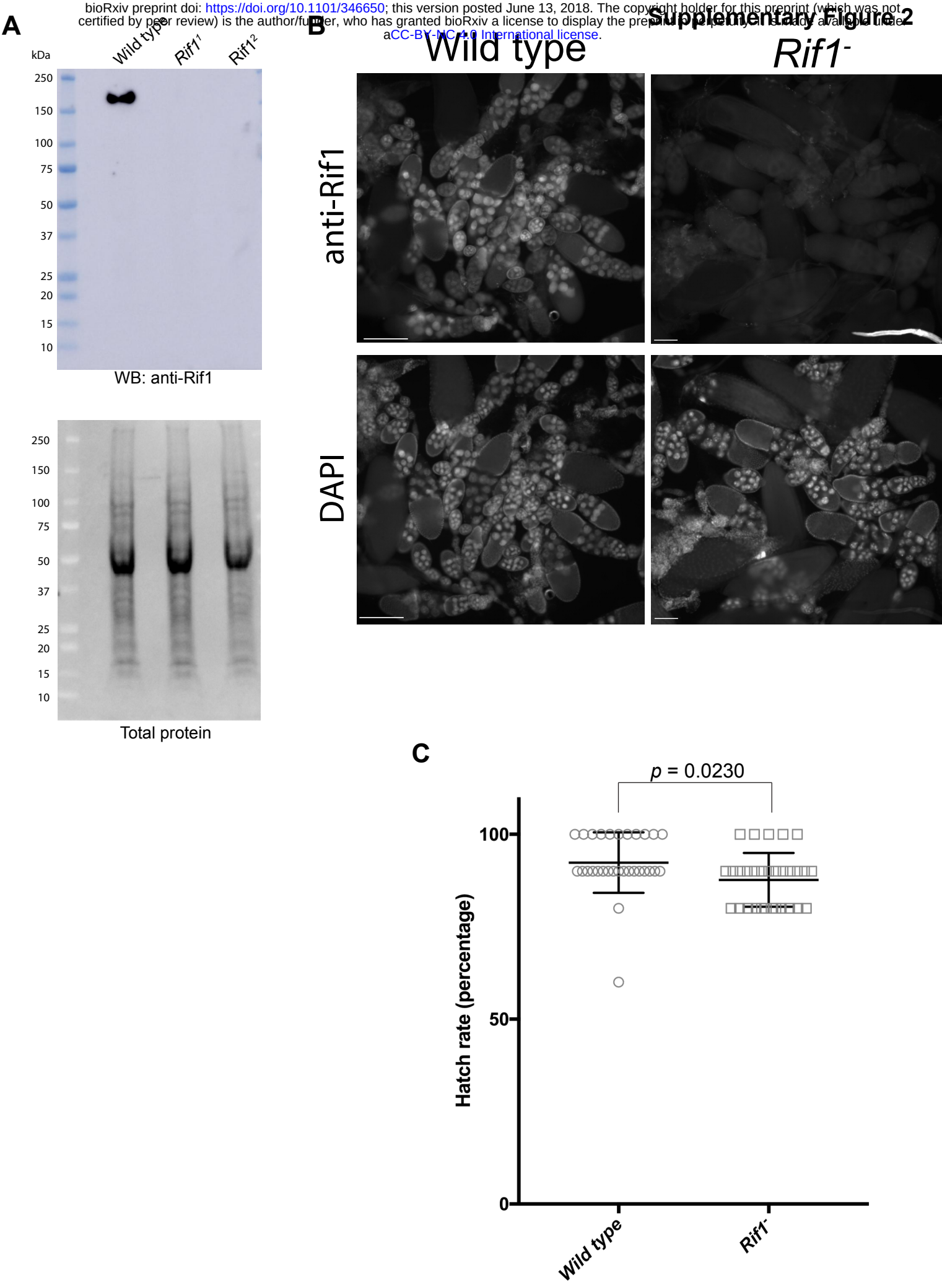

Supplementary Figure 3

A

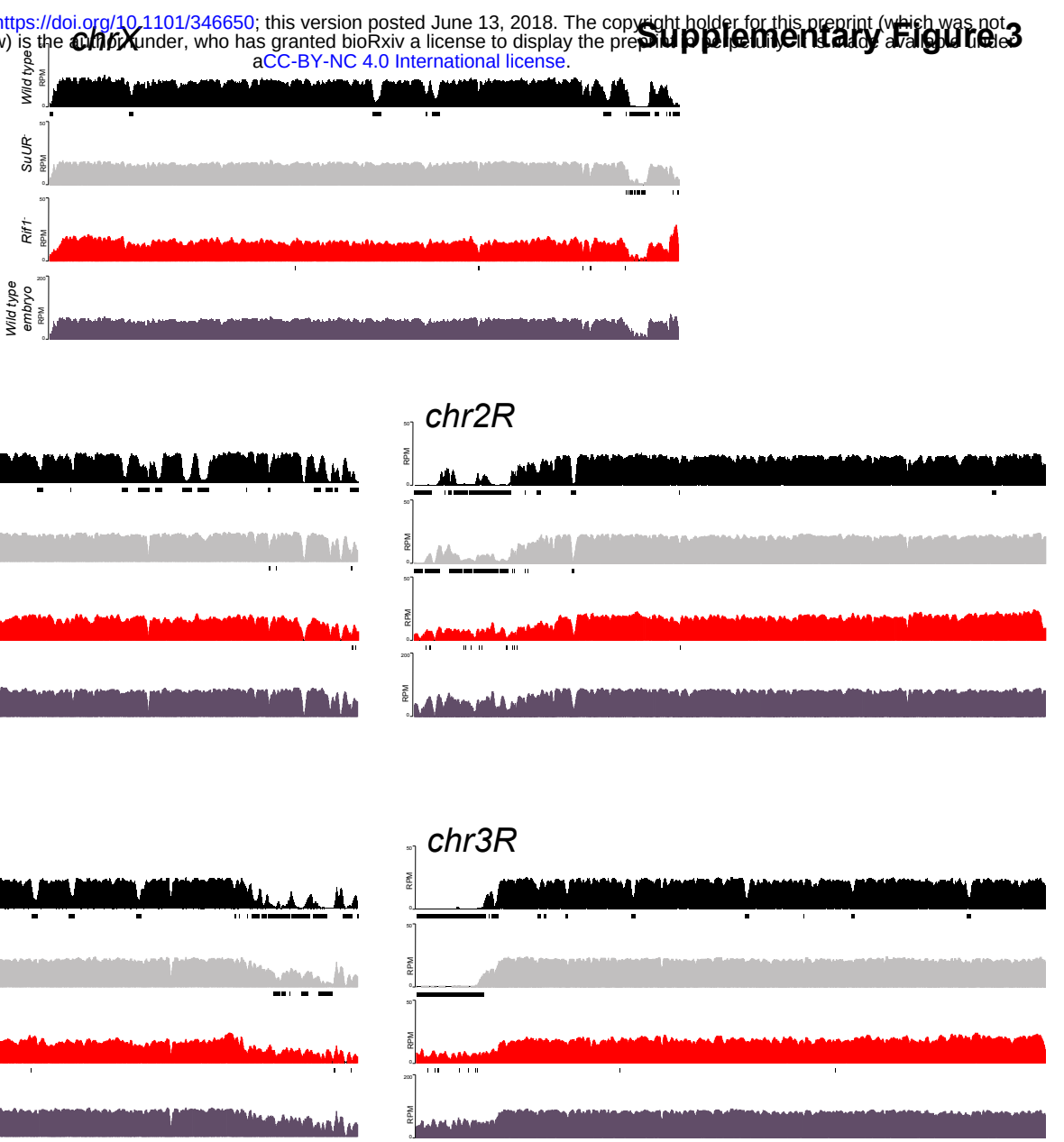

B

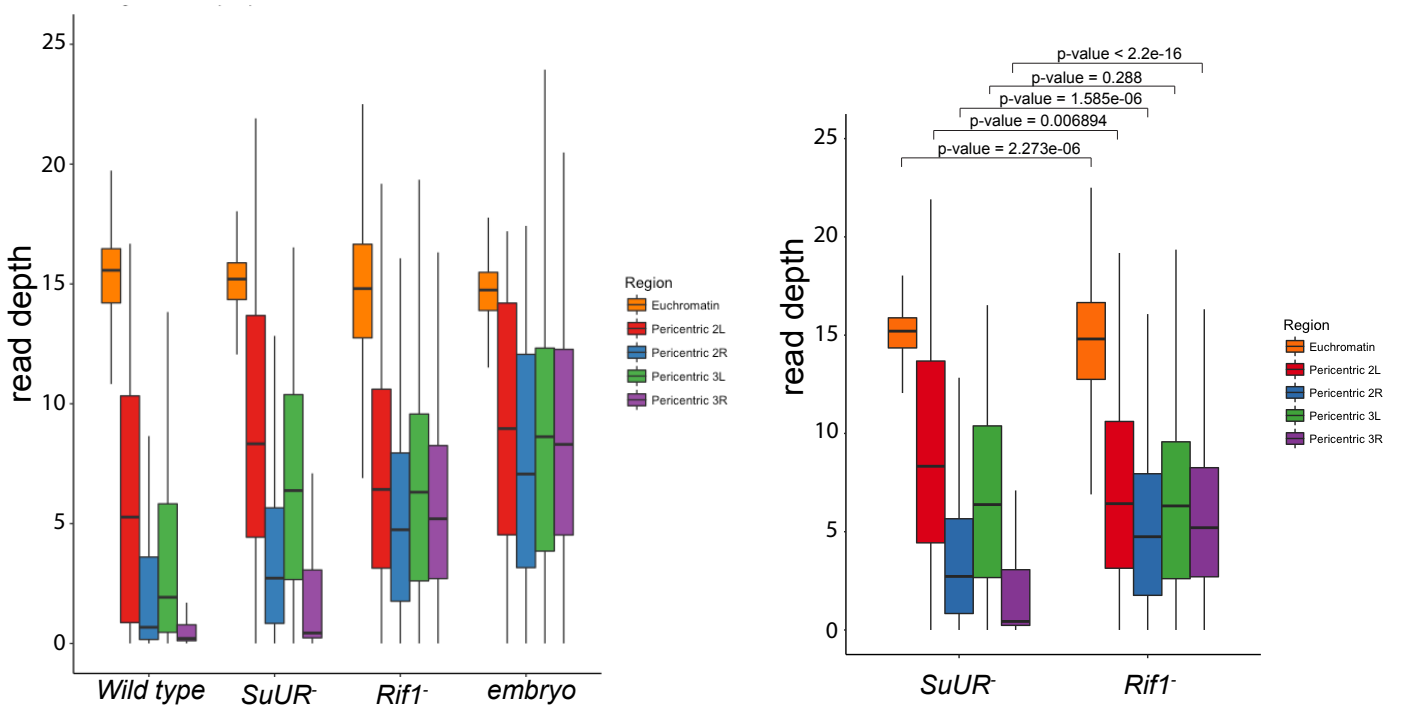

Supplementary Figure 4

A

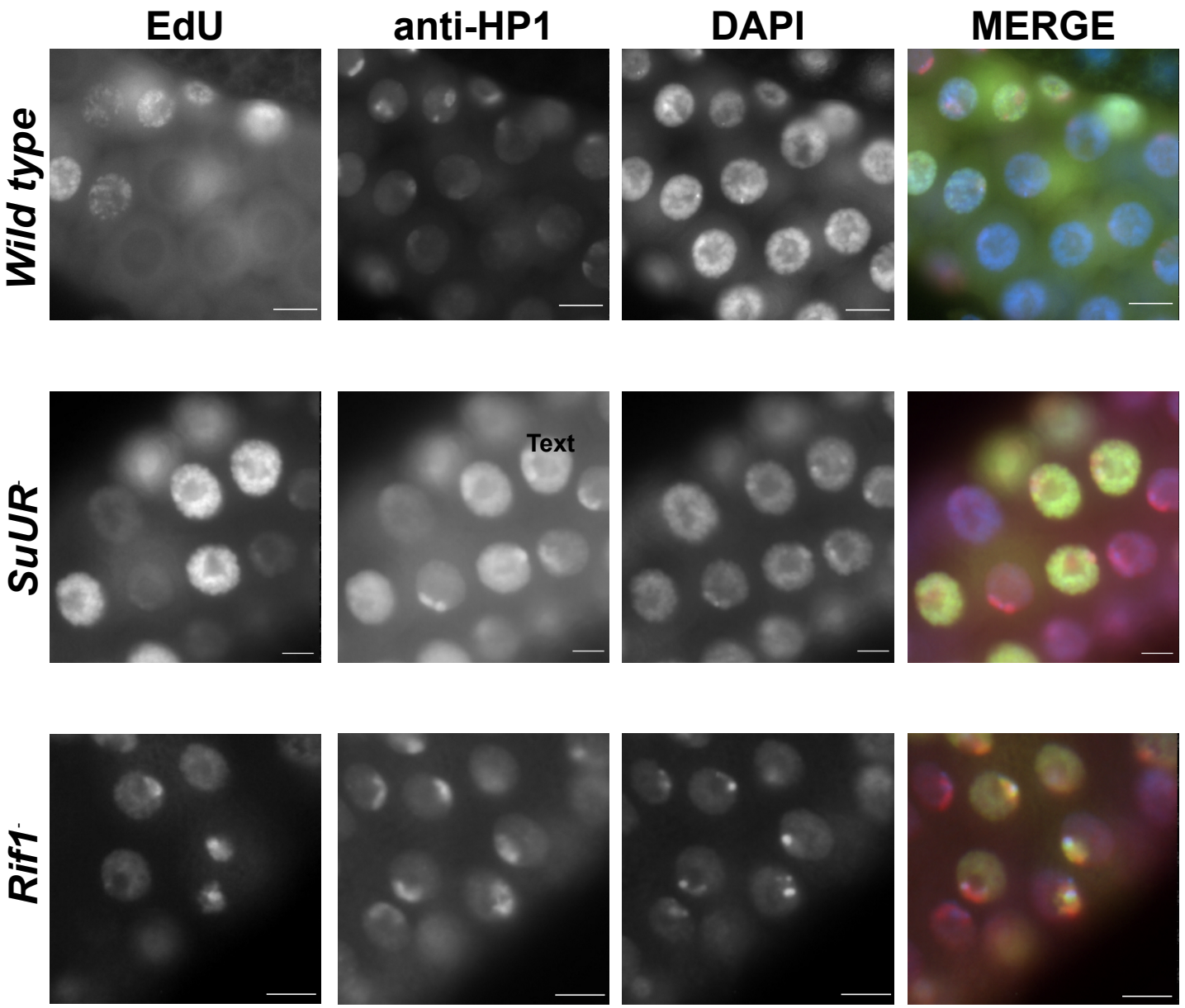

B

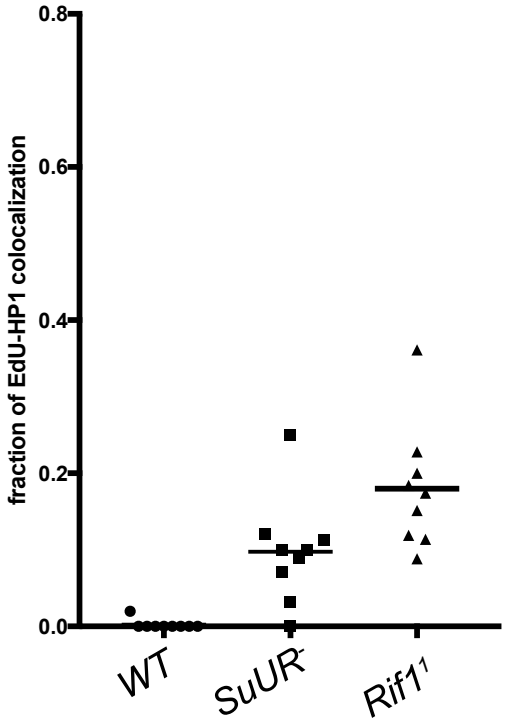

Supplementary Figure 5

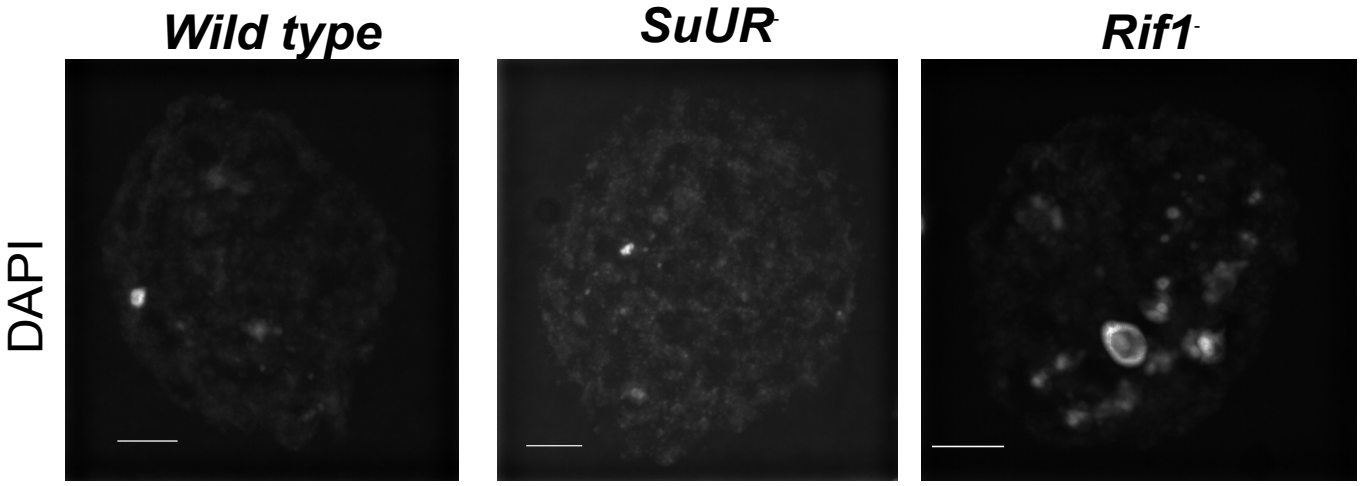

Supplementary Figure 6

A

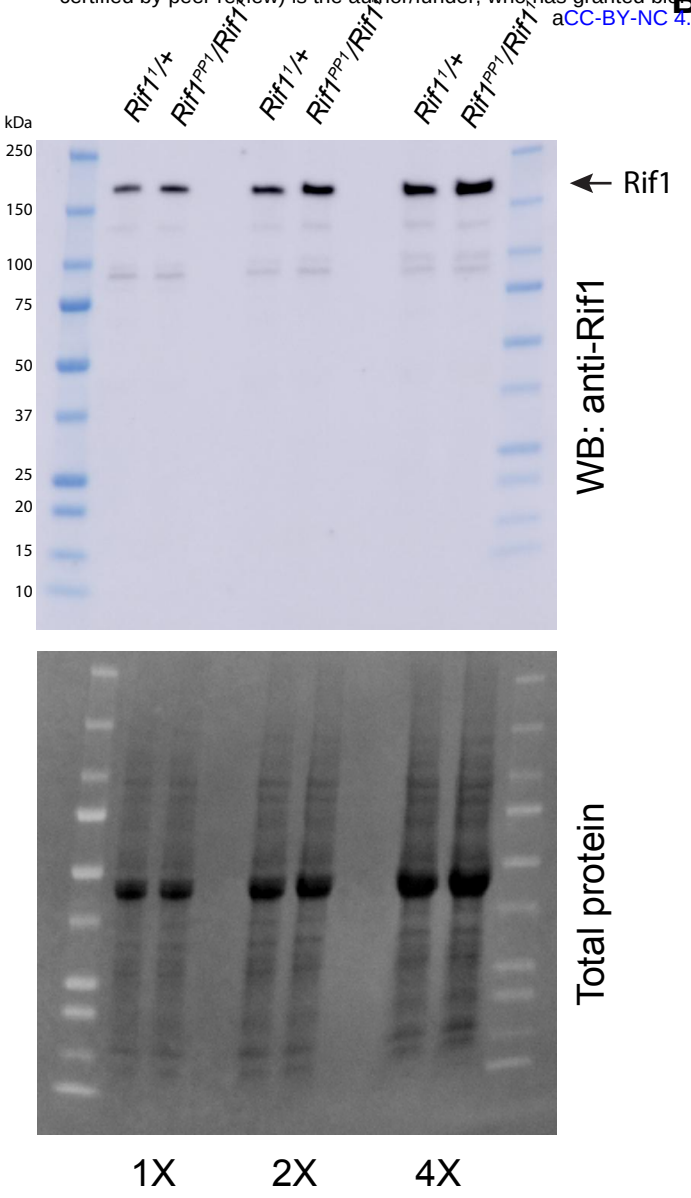

B

Supplemental Table 1: Underreplicated regions called by CNVnator

chr	start	end	OregonR	SuUR-	SuURΔSNF	Rif1-
chrX	9001	52000	+		+	
chrX	80001	108000	+			
chrX	2976001	3125000	+			
chrX	12052001	12382000	+			
chrX	14062001	14101000	+			
chrX	14292001	14563000	+			
chrX	20686001	20957000	+			
chrX	20962001	20998000	+			
chrX	21525001	21544000	+	+		+
chrX	21667001	21807000	+	+	+	
chrX	21814001	21829000	+			
chrX	21843001	21895000	+	+	+	
chrX	21904001	21965000	+	+	+	
chrX	21972001	22433000	+	+	+	
chrX	22611001	22787000	+	+		
chrX	23053001	23064000	+	+		
chrX	23175001	23205000	+			
chrX	23285001	23535000	+	+	+	
chr2L	4538001	4777000	+			
chr2L	8013001	8024000	+			
chr2L	11587001	11777000	+			
chr2L	12781001	12799000	+			
chr2L	14722001	14946000	+			
chr2L	15306001	15721000	+			
chr2L	15960001	16154000	+			
chr2L	16161001	16217000	+			
chr2L	16948001	17199000	+			
chr2L	17201001	17312000	+			
chr2L	17520001	17951000	+		+	
chr2L	19345001	19358000	+			
chr2L	20128001	20199000	+	+	+	
chr2L	21833001	22085000	+			
chr2L	22284001	22522000	+			
chr2L	22614001	22752000	+			
chr2L	23198001	23406000	+	+	+	+
chr2L	23415001	23513712	+		+	+
chr2R	1	699000	+	+	+	+
chr2R	1194001	1206000	+			
chr2R	1379001	1501000	+	+	+	
chr2R	1557001	1589000	+			

Supplementary Table 1 cont.

chr2R	1609001	1700000	+			
chr2R	1707001	1968000	+	+	+	
chr2R	1975001	2163000	+	+	+	+
chr2R	2170001	2409000	+	+	+	+
chr2R	2421001	2500000	+	+	+	
chr2R	2508001	2546000	+	+	+	
chr2R	2551001	3506000	+	+		+
chr2R	3513001	3871000	+	+	+	+
chr2R	4414001	4425000	+	+		
chr2R	4871001	5057000	+			
chr2R	6283001	6476000	+	+		
chr2R	10623001	10637000	+			+
chr2R	23133001	23313000	+			
chr3L	4850001	5034000	+			
chr3L	5043001	5075000	+			
chr3L	13559001	13805000	+			
chr3L	15196001	15475000	+			
chr3L	18190001	18431000	+			
chr3L	22577001	22627000	+			
chr3L	22803001	22820000	+			
chr3L	23157001	23173000	+		+	
chr3L	23355001	23538000	+			
chr3L	23550001	23679000	+			
chr3L	23775001	24005000	+			
chr3L	24056001	25075000	+	+	+	
chr3L	25135001	25838000	+	+	+	
chr3L	25844001	25965000	+		+	
chr3L	26085001	26161000	+		+	
chr3L	26166001	26311000	+	+		
chr3L	26315001	26705000	+	+	+	
chr3L	27391001	27815000	+			+
chr3L	28042001	28110227	+			
chr3R	1	1257000	+	+	+	+
chr3R	1266001	1655000	+	+		
chr3R	1664001	2569000	+	+	+	
chr3R	2572001	2824000	+	+	+	+
chr3R	2831001	3034000	+	+	+	+
chr3R	3040001	3129000	+	+		+
chr3R	3136001	3533000	+	+	+	
chr3R	3674001	3692000	+	+		
chr3R	3827001	3842000	+	+		
chr3R	3890001	4175000	+		+	

Supplementary Table 1 cont.

chr3R	6159001	6327000	+			
chr3R	6515001	6624000	+			
chr3R	7572001	7714000	+		+	
chr3R	10919001	11142000	+		+	
chr3R	16712001	16948000	+			
chr3R	19704001	19715000	+			
chr3R	22142001	22303000	+			+
chr3R	28020001	28252000	+			

Supplemental Table 2

			half max position			
Wild type		**max (log2)**	**left arm (bp)**	**right arm (bp)**	**half max total (bp)**	**fold change relative to wild type**
7F	*chrX*	*3.911*	8439400	8518500	79100	1
22B*	*chr2L*	*1.961*	1888300	1937200	48900	1
30B	*chr2L*	*1.798*	9504800	9587600	82800	1
34B	*chr2L*	*2.33*	13371800	13438500	66700	1
62D	*chr3L*	*1.678*	2231600	2314900	83300	1
66D	*chr3L*	*5.494*	8694700	8765800	71100	1

			half max position			
SuUR-		**max (log2)**	**left arm (bp)**	**right arm (bp)**	**half max total (bp)**	
7F	*chrX*	*3.528*	8425000	8528900	103900	1.313527181
22B*	*chr2L*	*NA*	NA	NA	NA	NA
30B	*chr2L*	*1.682*	9506100	9607700	101600	1.22705314
34B	*chr2L*	*2.355*	13364800	13473500	108700	1.629685157
62D	*chr3L*	*1.745*	2221200	2342400	121200	1.454981993
66D	*chr3L*	*4.88*	8685700	8778600	92900	1.306610408

			half max position			
Rif1-		**max (log2)**	**left arm (bp)**	**right arm (bp)**	**half max total (bp)**	
7F	*chrX*	*3.824*	8420700	8540700	120000	1.517067004
22B*	*chr2L*	*NA*	NA	NA	NA	NA
30B	*chr2L*	*1.807*	9496800	9607300	110500	1.334541063
34B	*chr2L*	*2.474*	13361400	13474400	113000	1.694152924
62D	*chr3L*	*1.719*	2217900	2335500	117600	1.411764706
66D	*chr3L*	*5.465*	8679700	8783500	103800	1.459915612

*22B is a strain specific amplicon present in Oregon R and not *SuUR* and *Rif1* mutants